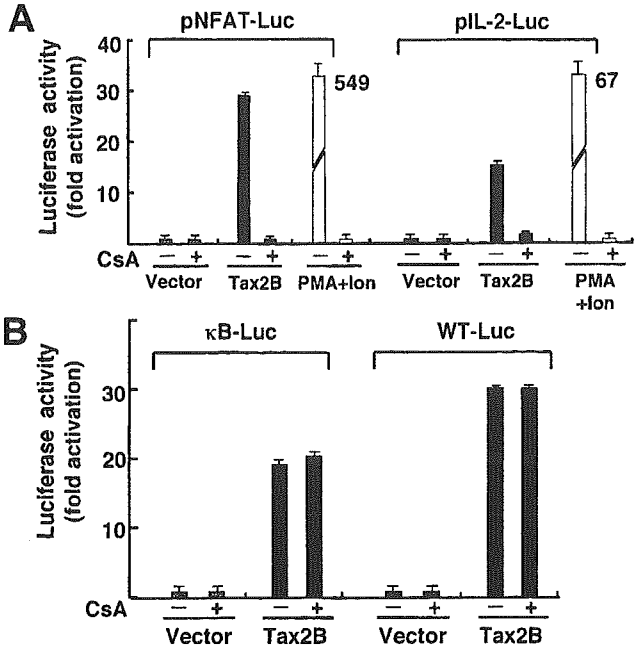

FIG. 6. Cyclosporine A inhibits the activation of NFAT by Tax2. (A and B) Jurkat cells (4×10^5 cells) were transfected with the indicated plasmids. At 42 h after transfection, the cells were treated with PMA and ionomycin or medium alone for 6 h. In addition, the Jurkat cells were treated with 0.2 μM of cyclosporine A (CsA) 0.5 h before treatment with PMA and ionomycin or treated with 0.2 μM of cyclosporine A 6 h after transfection with the *tax2* plasmid. Cell lysates were prepared and the luciferase and β-galactosidase activities were measured. Luciferase activity was normalized to that of β-galactosidase. The fold activation represents the luciferase activity of cells transfected with the *tax2* plasmid relative to that with the control plasmid. Error bars indicate standard deviations. Three independent experiments were carried out to confirm reproducibility.

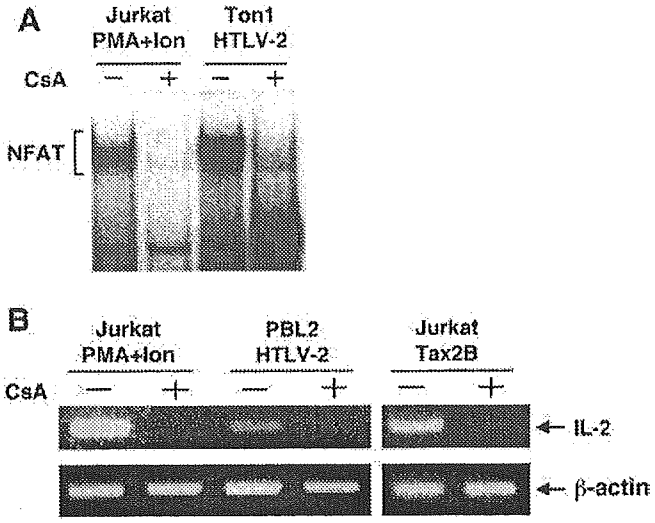

FIG. 7. Cyclosporine A inhibits the induction of IL-2 mRNA by Tax2 in T-cell lines. (A) Jurkat cells were treated with 20 ng/ml of PMA and 2 μM of ionomycin for 6 h together with 1 μM of cyclosporine A (CsA) for 6.5 h. Ton1 cells were treated with cyclosporine A for 24 h. Nuclear extracts were prepared from the cells and incubated with the NFAT site probe. Binding to the NFAT site probe was measured by EMSA as described in Materials and Methods. The position of the specific main complex with the NFAT element is indicated. The position of the NFAT complex is indicated. (B) Jurkat cells were either transfected with the *tax2B* plasmid or treated with PMA and ionomycin. Then, Jurkat and Ton1 cells were treated with 1 μM of cyclosporine A (CsA) for 6.5 h (Jurkat) and 24 h (Ton1). Total RNA was isolated and the RT-PCR products corresponding to IL-2 and β-actin mRNAs were amplified. The products were size-separated on a 2% agarose gel stained with ethidium bromide. The experiments were repeated three times to confirm reproducibility.

Cyclosporine A inhibits the activation of NFAT by Tax2. Cyclosporine A is a well-characterized inhibitor of the NFAT activation pathway (9). Cyclosporine A forms a complex with cyclophilin, and this complex specifically inhibits the activity of calcineurin, a calmodulin-dependent phosphatase. Calcineurin is required to dephosphorylate NFAT prior to its translocation to the nucleus. We next examined whether cyclosporine A could inhibit the activation of NFAT by Tax2.

Cyclosporine A potently inhibited the Tax2 activation of luciferase expression from pNFAT-Luc as well as that from pIL-2-Luc in Jurkat cells (Fig. 6A). The inhibition by cyclosporine A was specific to the activation of NFAT, since the activation of NF-κB (κB-Luc) and viral CRE (WT-Luc) by Tax2 was unaffected by cyclosporine A (Fig. 6B). Consistent with these results, cyclosporine A also inhibited nuclear NFAT localization in HTLV-2-infected cells (Ton1) as well as in Jurkat cells treated with PMA and ionomycin (Fig. 7A). In addition, cyclosporine A inhibited the inducible expression of IL-2 mRNA in HTLV-2-infected cells (PBL2) as well as in Jurkat cells transfected with the *tax2B* plasmid and in Jurkat cells treated with PMA and ionomycin (Fig. 7B). These results indicated that the activation of NFAT by Tax2 was sensitive to cyclosporine A inhibition, suggesting that Tax2 activates NFAT at the level at or upstream of the cyclophilin/calcineurin point of the signaling pathway.

Then, we examined whether NFAT activation in HTLV-2-infected cells regulates their growth. To check this, we cultured HTLV-2-infected cells in the presence or absence of cyclosporine A. PBL2 and PBL01 are IL-2-dependent HTLV-2-immortalized T-cell lines. These two cell lines still grew in the absence of IL-2, but overall cell growth was reduced by culture with cyclosporine A for 3 to 7 days (Fig. 8). However, growth inhibition by cyclosporine A was abrogated by the addition of IL-2 to the culture. On the other hand, cyclosporine A negligibly affected the growth of HTLV-uninfected cells (Jurkat) and an IL-2-dependent HTLV-1-infected T-cell line (ILT-Koy), in either the absence or presence of IL-2. These results suggested that constitutive activation of NFAT supports the cell growth of IL-2-dependent HTLV-2-infected cells in the absence of IL-2.

Unlike in IL-2-dependent cells, cyclosporine A did not inhibit the growth of two IL-2-independent HTLV-2-infected T-cell lines (Ton1 and MoT) in the presence or absence of IL-2. MoT was derived from a hairy cell leukemia patient, while Ton1 was established by in vitro transformation with lethally irradiated HTLV-2-infected T cells. It should be noted that IL-2-independent immortalization by HTLV-2 in vitro occurs much less frequently than IL-2-dependent immortalization. Thus, these IL-2-independent T-cell lines are likely to

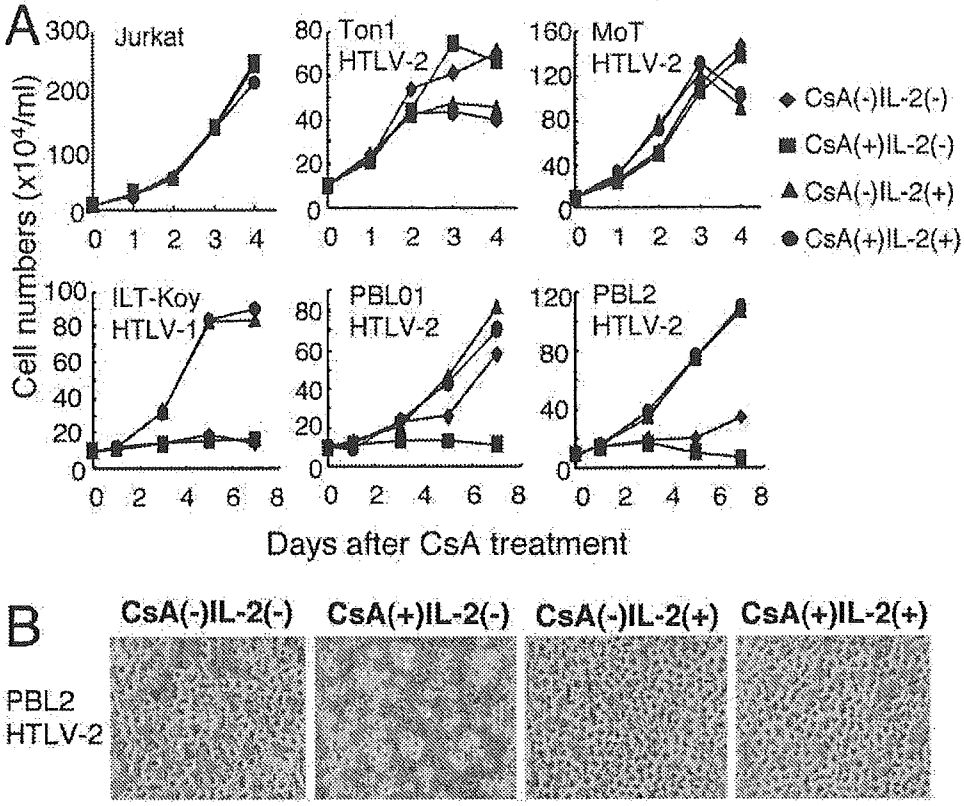

FIG. 8. Cyclosporine A inhibits growth of IL-2-dependent HTLV-2-infected cells. (A and B) The indicated T-cell lines were cultured in a combination of IL-2 and/or 0.5 μM of cyclosporine A (CsA) for 7 days. The number of viable cells (A) and the morphology of PBL2 cells at day 7 (B) were examined using a microscope. The experiments were repeated three times to confirm reproducibility.

have a genetic or epigenetic change(s), with such changes possibly conferring resistance to the inhibition of cell growth by cyclosporine A.

Finally, since NFAT regulates the induction of multiple cytokine genes, we examined whether IL-2 mediates the induced proliferation of HTLV-2-infected T-cell lines by Tax2 mediated through NFAT. For this purpose, two IL-2-dependent HTLV-2-infected T-cell lines, an IL-2-dependent HTLV-1-infected T-cell line, and IL-2-independent Jurkat cells were cultured in the absence of IL-2 and presence of two anti-IL-2 receptor antibodies (α-chain and β-chain), which can inhibit IL-2-dependent proliferation. Anti-IL-2 receptor antibodies reduced the growth only of the two HTLV-2-infected T-cell lines (Fig. 9). The effect of anti-IL-2 receptor antibodies was specific to HTLV-2-infected cell lines, since such cell growth inhibition was not observed for the HTLV-1-infected T-cell line or the Jurkat cell line. These results indicated that in HTLV-2-infected cells, induction of IL-2 production, mediated through NFAT activation, promotes proliferation.

DISCUSSION

Greene et al. reported that HTLV-2 Tax2 induces expression of IL-2 and IL-2R α-chain genes (13). However, whether induction of IL-2 gene expression plays a role in cell growth properties and phenotypes of HTLV-2-infected cells and how Tax2 activates IL-2 gene expression have not been characterized fully. In this study, we demonstrated that HTLV-2 Tax2 activated IL-2 gene expression, thereby promoting the proliferation of HTLV-2-infected T cells in the absence of IL-2. These results strongly suggest that an IL-2 autocrine loop is essential for maintaining the proliferation of HTLV-2-infected cells in low-IL-2 conditions in vitro as well as in vivo, thereby enabling establishment of life-long HTLV-2 infection. Unlike HTLV-2, HTLV-1 did not utilize the same IL-2 autocrine strategy for immortalization of T cells. These results suggest that immortalization of T cells by HTLV-2 through an IL-2 autocrine loop is a factor establishing a benign persistent infection which does not induce adult T-cell leukemia or related malignancies.

The anti-IL-2R β-chain antibody that we used here inhibits signaling by IL-15, which also promotes T-cell growth. Therefore, IL-15 may also be involved in the growth of HTLV-2-infected cells. Azimi et al. showed that HTLV-1 Tax1 induces the expression of IL-15 through NF-κB (5), but anti-IL-2R antibodies did not inhibit the growth or survival of HTLV-1-infected T cells (Fig. 9). Thus, it is unlikely that IL-15 is selectively involved in the growth of HTLV-2-infected cells but not HTLV-1-infected cells. Taken together, the experiments using anti-IL-2 receptor antibodies suggest that IL-2 produced from HTLV-2-infected T cells stimulates their growth.

IL-2 produced from HTLV-2-infected T-cell lines (PBL01 and PBL2) stimulated their growth but such IL-2 was not sufficient to support their continuous growth in vitro (Fig. 8

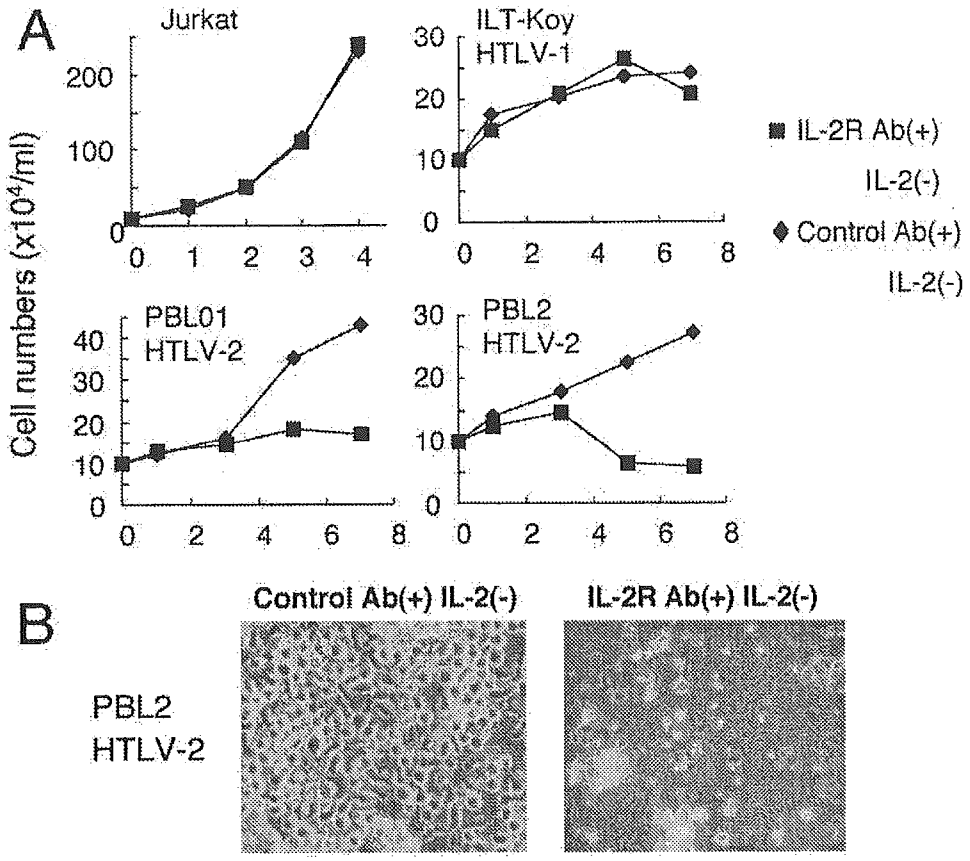

FIG. 9. Anti-IL-2R antibodies inhibit the growth of IL-2-dependent HTLV-2-infected cells. (A and B) The indicated T-cell lines were cultured in the absence of IL-2 together with anti-IL-2R antibodies (5 μg/ml of H31 and 5 μg/ml of TU27) or with 10 μg/ml of control antibody for 7 days. The number of viable cells (A) and the morphology of PBL2 cells at day 7 (B) were examined using a microscope. The experiments were repeated three times to confirm reproducibility.

and 9). Thus, it is unclear whether IL-2 produced from HTLV-2-infected T-cell lines is sufficient for their continuous survival and cell growth in vivo. IL-2 induction by Tax2 was synergistically enhanced in Jurkat cells treated with PMA and ionomycin (data not shown), suggesting that antigen stimulation and Tax2 cooperatively induce the production of IL-2 in HTLV-2-infected T cells, which may fully support the survival and growth of HTLV-2-infected T cells in vivo. Further studies are, however, required to establish to what extent IL-2 contributes to the long-term survival and cell growth of HTLV-2-infected T cells in vivo.

There is no substantial evidence that growth of HTLV-1-infected cells is regulated by autocrine factors, including IL-2 (3, 39). Instead, several studies suggested that intracellular Tax1 directly attacks the host cell cycle machinery through a protein-protein interaction to promote cell growth. For instance, Tax1 interacts with several cell cycle regulators such as p16INK4A and CDK4, and the interactions are correlated with the cell cycle promotion induced by Tax1 (14, 35). HTLV-1-infected cells accumulate multiple genetic and epigenetic changes before adult T-cell leukemia development. Thus, the autocrine promotion of cell proliferation by HTLV-2 may result in less accumulation of genetic and/or epigenetic changes in infected cells.

In activated T cells, NFATp binds to the NFAT site on the IL-2 promoter as a complex with another transcription factor, AP-1 (6). AP-1 is a heterodimer or homodimer of Jun and Fos family members, and Tax1 activates AP-1-dependent transcription through inducing the expression of various AP-1 family members (11, 17). Stimulation via AP-1 does not, however, account for the differences in the interaction of Tax2 and Tax1 with the IL-2 NFAT site, since both Tax1 and Tax2 activate AP-1-dependent transcription, and their activities were equivalent (data not shown).

Experiments using chimeric Tax proteins indicated that the Tax2B amino acid region between 60 and 300 included a factor required for the augmented NFAT activity. Since this region in Tax2B and Tax2A differs by only one amino acid, the conserved amino acid variation(s) of Tax2B and Tax2A relative to Tax1 must account for the differences in NFAT activity. We are comprehensively delineating the domain of Tax2 responsible for this activity. As a next step, we will examine whether this Tax2-specific function is involved in the immortalization of primary T cells as well as persistent HTLV-2 infection in rabbit or rat model systems using a molecular clone of HTLV-2.

Several differences between Tax1 and Tax2 have been identified. For instance, Tax1 has greater transforming activity toward the Rat-1 fibroblast cell line (measured as colony formation in soft agar) than Tax2, and this difference is mediated by a PDZ domain binding motif (PBM) in Tax1, which is missing

in Tax2. Since the PBM is localized at the C-terminal end of Tax1, PBM does not explain the reduced NFAT activation by Tax1 (16). Second, when the expression plasmids were transfected into a cell line, Tax2 localized in the cytoplasm while Tax1 localized in the nucleus (26). Thus, multiple differences between Tax1 and Tax2, including the activation of NFAT, are probably involved in the distinct pathogenesis of HTLV-1 and HTLV-2. Thus, further analysis is required to understand how the distinct pathogenesis of two related viruses is determined.

While NFAT, AP-1, and NF-κB are constitutively active in HTLV-2-infected cells, only AP-1 and NF-κB are constitutively activated in HTLV-1-infected cells. These three transcription factors are critical components of T-cell activation, differentiation, and proliferation during immune activation. These functions are carried out mainly through regulation of cytokine gene expression. Specifically, NFAT and AP-1 interact with each other to cooperatively regulate the expression of several cytokines, including IL-2, during an immune response (23). Thus, individuals infected with HTLV-1 and HTLV-2 would have distinct long-term cytokine profiles during persistent infection. Consequently, such distinct cytokine production may alter the immune status of HTLV infection, thereby being a factor responsible for the different modes of pathogenesis of HTLV-1 and HTLV-2.

In addition to adult T-cell leukemia, HTLV-1 is associated with several chronic inflammatory diseases such as HTLV-1-associated myelopathy/tropical spastic paraparesis and HTLV-1-associated uveitis. While HTLV-2 infection is not associated with development of adult T-cell leukemia, recent results suggest that HTLV-2 is associated with HTLV-1-associated myelopathy/tropical spastic paraparesis. Thus, cyclosporine A and anti-IL-2 receptor antibodies, especially cyclosporine A or related NFAT inhibitors, may be promising candidates for therapeutics for HTLV-2-associated diseases.

ACKNOWLEDGMENTS

This work was supported in part by a Grant-in-Aid for Scientific Research on Priority Areas (C) and for Scientific Research (C) of Japan and grants from the National Institutes of Health (CA77556 and CA92009).

We thank William W. Hall and Mari Kannagi for the Tax2B plasmid, the antibody against Tax2B, and the HTLV-1-infected T-cell lines. We thank the Takeda pharmaceutical company for providing recombinant human IL-2. We also thank Sayoko Takizawa and Chika Yamamoto for excellent technical assistance and Kathleen Hayes for assistance in editing the manuscript.

REFERENCES

1. **Akagi, T., H. Ono, N. Tsuchida, and K. Shimotohno.** 1997. Aberrant expression and function of p53 in T cells immortalized by HTLV-I Tax1. FEBS Lett. **406**:263–266.
2. **Akagi, T., and K. Shimotohno.** 1993. Proliferative response of Tax1-transduced primary human T cells to anti-CD3 antibody stimulation by an interleukin-2-independent pathway. J. Virol. **67**:1211–1217.
3. **Arya, S. K., F. Wong-Staal, and R. C. Gallo.** 1984. T-cell growth factor gene: lack of expression in human T-cell leukemia-lymphoma virus-infected cells. Science **223**:1086–1087.
4. **Asada, H., N. Ishii, Y. Sasaki, K. Endo, H. Kasai, N. Tanaka, T. Takeshita, S. Tsuchiya, T. Konno, and K. Sugamura.** 1999. Grf40, A novel Grb2 family member, is involved in T-cell signaling through interaction with SLP-76 and LAT. J. Exp. Med. **189**:1383–1390.
5. **Azimi, N., K. Brown, R. N. Bamford, Y. Tagaya, U. Siebenlist, and T. A. Waldmann.** 1998. Human T-cell lymphotropic virus type I Tax protein transactivates interleukin 15 gene transcription through an NF-kappaB site. Proc. Natl. Acad. Sci. USA **95**:2452–2457.
6. **Boise, L. H., B. Petryniak, X. Mao, C. H. June, C. Y. Wang, T. Lindsten, R. Bravo, K. Kovary, J. M. Leiden, and C. B. Thompson.** 1993. The NFAT-1 DNA binding complex in activated T cells contains Fra-1 and JunB. Mol. Cell. Biol. **13**:1911–1919.
7. **Chen, I. S., J. McLaughlin, J. C. Gasson, S. C. Clark, and D. W. Golde.** 1983. Molecular characterization of genome of a novel human T-cell leukaemia virus. Nature **305**:502–505.
8. **Chen, I. S., S. G. Quan, and D. W. Golde.** 1983. Human T-cell leukemia virus type II transforms normal human lymphocytes. Proc. Natl. Acad. Sci. USA **80**:7006–7009.
9. **Clipstone, N. A., and G. R. Crabtree.** 1992. Identification of calcineurin as a key signalling enzyme in T-lymphocyte activation. Nature **357**:695–697.
10. **Cross, S. L., M. B. Feinberg, J. B. Wolf, N. J. Holbrook, F. Wong-Staal, and W. J. Leonard.** 1987. Regulation of the human interleukin-2 receptor alpha chain promoter: activation of a nonfunctional promoter by the transactivator gene of HTLV-I. Cell **49**:47–56.
11. **Fujii, M., T. Niki, T. Mori, T. Matsuda, M. Matsui, N. Nomura, and M. Seiki.** 1991. HTLV-1 Tax induces expression of various immediate early serum responsive genes. Oncogene **6**:1023–1029.
12. **Grassmann, R., S. Berchtold, I. Radant, M. Alt, B. Fleckenstein, J. G. Sodroski, W. A. Haseltine, and U. Ramstedt.** 1992. Role of human T-cell leukemia virus type 1 X region proteins in immortalization of primary human lymphocytes in culture. J. Virol. **66**:4570–4575.
13. **Greene, W. C., W. J. Leonard, Y. Wano, P. B. Svetlik, N. J. Peffer, J. G. Sodroski, C. A. Rosen, W. C. Goh, and W. A. Haseltine.** 1986. Trans-activator gene of HTLV-II induces IL-2 receptor and IL-2 cellular gene expression. Science **232**:877–880.
14. **Haller, K., Y. Wu, E. Derow, I. Schmitt, K. T. Jeang, and R. Grassmann.** 2002. Physical interaction of human T-cell leukemia virus type 1 Tax with cyclin-dependent kinase 4 stimulates the phosphorylation of retinoblastoma protein. Mol. Cell. Biol. **22**:3327–3338.
15. **Hinuma, Y., K. Nagata, M. Hanaoka, M. Nakai, T. Matsumoto, K. I. Kinoshita, S. Shirakawa, and I. Miyoshi.** 1981. Adult T-cell leukemia: antigen in an ATL cell line and detection of antibodies to the antigen in human sera. Proc. Natl. Acad. Sci. USA **78**:6476–6480.
16. **Hirata, A., M. Higuchi, A. Niinuma, M. Ohashi, M. Fukushi, M. Oie, M. Akiyama, Y. Tanaka, F. Gejyo, and M. Fujii.** 2004. PDZ domain-binding motif of human T-cell leukemia virus type 1 Tax oncoprotein augments the transforming activity in a rat fibroblast cell line. Virology **318**:327–336.
17. **Iwai, K., N. Mori, M. Oie, N. Yamamoto, and M. Fujii.** 2001. Human T-cell leukemia virus type 1 tax protein activates transcription through AP-1 site by inducing DNA binding activity in T cells. Virology **279**:38–46.
18. **Iwanaga, Y., Tsukahara.T., T. Ohashi, Y. Tanaka, M. Araii, M. Nakamura, K. Ohtani, Y. Koya, M. Kannagi, N. Yamamoto, and M. Fujii.** 1999. Human T-cell leukemia virus type 1 Tax protein abrogates interleukin 2 dependence in a mouse T-cell line. J. Virol. **73**:1271–1277.
19. **Jin, D. Y., F. Spencer, and K. T. Jeang.** 1998. Human T-cell leukemia virus type 1 oncoprotein Tax targets the human mitotic checkpoint protein MAD1. Cell **93**:81–91.
20. **Katsuki, T., K. Katsuki, J. Imai, and Y. Hinuma.** 1987. Immune suppression in healthy carriers of adult T-cell leukemia retrovirus (HTLV-I): impairment of T-cell control of Epstein-Barr virus-infected B-cells. Jpn. J. Cancer Res. **78**:639–642.
21. **Lee, H. J., N. Koyano-Nakagawa, Y. Naito, J. Nishida, N. Arai, K. Arai, and T. Yokota.** 1993. cAMP activates the IL-5 promoter synergistically with phorbol ester through the signaling pathway involving protein kinase A in mouse thymoma line EL-4. J. Immunol. **151**:6135–6142.
22. **Lewis, M. J., P. Novoa, R. Ishak, M. Ishak, M. Salemi, A. M. Vandamme, M. H. Kaplan, and W. W. Hall.** 2000. Isolation, cloning, and complete nucleotide sequence of a phenotypically distinct Brazilian isolate of human T-lymphotropic virus type II (HTLV-II). Virology **271**:142–154.
23. **Macian, F., C. Lopez-Rodriguez, and A. Rao.** 2001. Partners in transcription: NFAT and AP-1. Oncogene **20**:2476–2489.
24. **Maruyama, M., H. Shibuya, H. Harada, M. Hatakeyama, M. Seiki, T. Fujita, J. Inoue, M. Yoshida, and T. Taniguchi.** 1987. Evidence for aberrant activation of the interleukin-2 autocrine loop by HTLV-I-encoded p40^{x} and T3/Ti complex triggering. Cell **48**:343–350.
25. **Matsuoka, M.** 2003. Human T-cell leukemia virus type I and adult T-cell leukemia. Oncogene **22**:5131–5140.
26. **Meertens, L., S. Chevalier, R. Weil, A. Gessain, and R. Mahieux.** 2004. A 10-amino acid domain within human T-cell leukemia virus type 1 and type 2 tax protein sequences is responsible for their divergent subcellular distribution. J. Biol. Chem. **279**:43307–43320.
27. **Miyoshi, I., I. Kubonishi, S. Yoshimoto, T. Akagi, Y. Ohtsuki, Y. Shiraishi, K. Nagata, and Y. Hinuma.** 1981. Type C virus particles in a cord T-cell line derived by co-cultivating normal human cord leukocytes and human leukaemic T cells. Nature **294**:770–771.
28. **Northrop, J. P., K. S. Ullman, and G. R. Crabtree.** 1993. Characterization of the nuclear and cytoplasmic components of the lymphoid-specific nuclear factor of activated T cells (NF-AT) complex. J. Biol. Chem. **268**:2917–2923.
29. **Pise-Masison, C. A., K. S. Choi, M. Radonovich, J. Dittmer, S. J. Kim, and J. N. Brady.** 1998. Inhibition of p53 transactivation function by the human T-cell lymphotropic virus type 1 Tax protein. J. Virol. **72**:1165–1170.

30. **Poiesz, B. J., F. W. Ruscetti, A. F. Gazdar, P. A. Bunn, J. D. Minna, and R. C. Gallo.** 1980. Detection and isolation of type C retrovirus particles from fresh and cultured lymphocytes of a patient with cutaneous T-cell lymphoma. Proc. Natl. Acad. Sci. USA **77**:7415–7419.
31. **Robek, M. D., and L. Ratner.** 1999. Immortalization of CD4(+) and CD8(+) T lymphocytes by human T-cell leukemia virus type 1 Tax mutants expressed in a functional molecular clone. J. Virol. **73**:4856–4865.
32. **Ross, T. M., S. M. Pettiford, and P. L. Green.** 1996. The tax gene of human T-cell leukemia virus type 2 is essential for transformation of human T lymphocytes. J. Virol. **70**:5194–5202.
33. **Seiki, M., S. Hattori, Y. Hirayama, and M. Yoshida.** 1983. Hum. adult T-cell leukemia virus: Complete nucleotide sequence of the provirus genome integrated in leukemia cell DNA. Proc. Natl. Acad. Sci. USA **80**:3618–3622.
34. **Sugamura, K., and Y. Hinuma.** 1993. Human retroviruses: HTLV-I and HTLV-II, p. 399–435. In J. A. Levy (ed.), The *Retroviridae*, vol. 2. Plenum Press, New York, NY.
35. **Suzuki, T., S. Kitao, H. Matsushime, and M. Yoshida.** 1996. HTLV-1 Tax protein interacts with cyclin-dependent kinase inhibitor p16INK4A and counteracts its inhibitory activity towards CDK4. EMBO J. **15**:1607–1614.
36. **Takeshita, T., Y. Goto, K. Tada, K. Nagata, H. Asao, and K. Sugamura.** 1989. Monoclonal antibody defining a molecule possibly identical to the p75 subunit of interleukin 2 receptor. J. Exp. Med. **169**:1323–1332.
37. **Tanaka, Y., A. Yoshida, H. Tozawa, H. Shida, H. Nyunoya, and K. Shimotohno.** 1991. Production of a recombinant human T-cell leukemia virus type-I trans-activator (tax1) antigen and its utilization for generation of monoclonal antibodies against various epitopes on the tax1 antigen. Int. J. Cancer **48**:623–630.
38. **Uchiyama, T., J. Yodoi, K. Sagawa, K. Takatsuki, and H. Uchino.** 1977. Adult T-cell leukemia: clinical and hematologic features of 16 cases. Blood **50**:481–492.
39. **Volkman, D. J., M. Popovic, R. C. Gallo, and A. S. Fauci.** 1985. Human T-cell leukemia/lymphoma virus-infected antigen-specific T-cell clones: indiscriminant helper function and lymphokine production. J. Immunol. **134**:4237–4243.
40. **Winslow, M. M., J. R. Neilson, and G. R. Crabtree.** 2003. Calcium signalling in lymphocytes. Curr. Opin. Immunol. **15**:299–307.
41. **Yamamoto, N., M. Okada, Y. Koyanagi, M. Kannagi, and Y. Hinuma.** 1982. Transformation of human leukocytes by cocultivation with an adult T-cell leukemia virus producer cell line. Science **217**:737–739.
42. **Zhao, L. J., and C. Z. Giam.** 1992. Human T-cell lymphotropic virus type I (HTLV-I) transcriptional activator, Tax, enhances CREB binding to HTLV-I 21-base-pair repeats by protein-protein interaction. Proc. Natl. Acad. Sci. USA **89**:7070–7074.

During Viral Infection of the Respiratory Tract, CD27, 4-1BB, and OX40 Collectively Determine Formation of CD8$^+$ Memory T Cells and Their Capacity for Secondary Expansion[1]

Jenny Hendriks,* Yanling Xiao,* John W. A. Rossen,† Koenraad F. van der Sluijs,‡ Kazuo Sugamura,§ Naoto Ishii,§ and Jannie Borst[2]*

Independent studies have shown that CD27, 4-1BB, and OX40 can all promote survival of activated CD8$^+$ T cells. We have therefore compared their impact on CD8$^+$ memory T cell formation and responsiveness within one, physiologically relevant model system. Recombinant mice, selectively lacking input of one or two receptors, were challenged intranasally with influenza virus, and the immunodominant virus-specific CD8$^+$ T cell response was quantified at priming and effector sites. Upon primary infection, CD27 and (to a lesser extent) 4-1BB made nonredundant contributions to accumulation of CD8$^+$ virus-specific T cells in draining lymph nodes and lung, while OX40 had no effect. Interestingly though, in the memory response, accumulation of virus-specific CD8$^+$ T cells in spleen and lung critically depended on all three receptor systems. This was explained by two observations: 1) CD27, 4-1BB, and OX40 were collectively responsible for generation of the same memory CD8$^+$ T cell pool; 2) CD27, 4-1BB, and OX40 collectively determined the extent of secondary expansion, as shown by adoptive transfers with standardized numbers of memory cells. Surprisingly, wild-type CD8$^+$ memory T cells expanded normally in primed OX40 ligand- or 4-1BB ligand-deficient mice. However, when wild-type memory cells were generated in OX40 ligand- or 4-1BB ligand-deficient mice, their secondary expansion was impaired. This provides the novel concept that stimulation of CD8$^+$ T cells by OX40 and 4-1BB ligand during priming imprints into them the capacity for secondary expansion. Our data argue that ligand on dendritic cells and/or B cells may be critical for this. *The Journal of Immunology,* **2005, 175: 1665–1676.**

An effective immune response relies on the clonal amplification of Ag-specific T cells and their accumulation at the site of infection. For long-term protection, part of the Ag-specific T cell pool must be retained as memory cells, which respond rapidly to renewed challenge. Naive T cell expansion is initiated by TCR signaling, but this alone is not sufficient. Costimulatory receptors must be engaged, which promote T cell division and survival and may direct development of effector functions. Costimulatory receptors comprise Ig superfamily members, including CD28 and ICOS, and TNFR family members, such as CD27, 4-1BB, and OX40 (1, 2). Like the TCR, CD28 and relatives signal via tyrosine kinases, while costimulatory TNFR family members signal via TNFR-associated factors (3). Both mechanisms activate the NF-κB and Jun kinase pathways, posing the question as to whether signals provided by the various costimulatory receptors merely add to TCR signaling and to each other in quantitative terms.

Previously, we have determined that CD27 gives a critical survival signal to activated T cells (4). Upon intranasal infection with influenza virus, CD27 and CD28 equally contributed to expansion of virus-specific CD8$^+$ T cells and their accumulation at the effector site. Unlike CD28, CD27 did not affect cell cycle entry or activity. Rather, CD27 protected primed T cells from apoptosis (4) and appeared to complement CD28 in its antiapoptotic effect (5). 4-1BB and OX40, the closest relatives of CD27 (1, 2), also promote activated T cell survival, apparently by stimulating expression of inhibitory Bcl-2 family members (6, 7). Although this suggests redundancy between CD27, 4-1BB, and OX40, complementarity may lie in their selective effects on certain cell populations and the timing of their involvement. The expression patterns of these receptors give a clue that this might be the case. CD27 is already expressed on naive T cells (8, 9), but 4-1BB and OX40 are induced by TCR signals, with CD28 enhancing their expression (6, 10–12). Accordingly, in activated T cells lacking 4-1BB or OX40 signaling, survival is not compromised initially, but it is defective in the later divisions (6, 13).

The ligands are TNF-related transmembrane molecules, which emerge transiently, under strict control of Ag receptors and TLRs (3, 8). CD70, the ligand of CD27, 4-1BB ligand (4-1BBL),[3] and OX40 ligand (OX40L) have all been found on activated lymphocytes and mature dendritic cells (DC) (10, 14–17), indicating that receptor/ligand interactions come into play during communication between T cells and APCs as well as among effector T cells. Limited data are available on their expression in vivo. Deliberate constitutive expression of CD70, 4-1BBL, or OX40L by transgenesis upsets lymphocyte homeostasis, leading to immunodeficiency or autoimmunity, indicating that the transient availability of these ligands is crucial to prevent pathogenesis (18–21).

*Division of Immunology, The Netherlands Cancer Institute, Amsterdam, The Netherlands; †Department of Virology, University Medical Center, Utrecht, The Netherlands; ‡Department of Pulmonology and Laboratory of Experimental Immunology, Academic Medical Center, Amsterdam, The Netherlands; and §Department of Microbiology and Immunology, Tohoku University Graduate School of Medicine, Sendai, Japan

Received for publication September 7, 2004. Accepted for publication May 24, 2005.

The costs of publication of this article were defrayed in part by the payment of page charges. This article must therefore be hereby marked *advertisement* in accordance with 18 U.S.C. Section 1734 solely to indicate this fact.

[1] This work was supported by The Netherlands Organization for Scientific Research and the Dutch Cancer Society.

[2] Address correspondence and reprint requests to Dr. Jannie Borst, Division of Immunology, The Netherlands Cancer Institute, Plesmanlaan 121, 1066 CX Amsterdam, The Netherlands. E-mail address: j.borst@nki.nl

[3] Abbreviations used in this paper: 4-1BBL, 4-1BB ligand; DC, dendritic cell; DLN, draining lymph node; NP, nuclear protein; OX40L, OX40 ligand.

0022-1767/05/$02.00

Phenotypes of receptor- and ligand-deficient mice are subtle as compared with phenotypes of mice in which the receptors are deliberately stimulated. Agonistic anti-4-1BB or anti-OX40 Abs rescued T cells from activation-induced cell death and promoted memory formation (22, 23). In CD70 transgenic mice, effector CD4$^+$ and CD8$^+$ T cells develop in the absence of deliberate antigenic challenge (18, 19), and in nonimmunized OX40L transgenic mice, CD4$^+$ effector T cells accumulate (20). In addition, in CD70 transgenic mice, CD8$^+$ effector T cells, and in OX40L transgenic mice, CD4$^+$ effector T cells showed decreased contraction after antigenic challenge (20, 24).

Like the studies with deliberate receptor triggering, initial analysis of receptor- and ligand-deficient mice suggested that 4-1BB and OX40 selectively impact on CD8$^+$ and CD4$^+$ effector T cells, respectively, while CD27 impacts on both. In CD27$^{-/-}$ mice infected intranasally with influenza virus, accumulation of both CD4$^+$ and CD8$^+$ effector T cells was reduced (25). In mice lacking 4-1BBL, fewer CD8$^+$ effector T cells and memory T cells developed upon i.p. challenge with influenza virus (26–28). OX40- and OX40L-deficient mice had reduced primary CD4$^+$ T cell responses to intranasal virus and to protein Ags (29–31). Lower frequencies of effector CD4$^+$ T cells were generated late in the primary response, and fewer CD4$^+$ memory T cells developed (32). However, recent work indicates that this specialization is not absolute: OX40 can promote primary CD8 T cell responses (33, 34) by supporting CD8$^+$ T cell survival (34).

There are many data on the role of costimulatory receptors in primary responses, but less is known about their importance for memory responses. In our model of intranasal delivery of influenza virus, accumulation of CD8$^+$ effector T cells in the memory response critically depended on both CD27 and CD28 (4, 25). Upon i.p. delivery of influenza virus, 4-1BBL$^{-/-}$ and OX40L$^{-/-}$ mice were selectively impaired in CD8$^+$ and CD4$^+$ memory T cell responses, respectively (28, 35). In a model of virus-induced lung inflammation, OX40 also controlled accumulation of CD4$^+$ effector cells in the memory response (33, 36). These data suggest that CD27 and 4-1BB are important for antiviral CD8$^+$ memory responses, while OX40 is not.

In this study, we used recombinant mice deficient for CD27, 4-1BB, and/or OX40 signaling to address the question as to whether these receptors make complementary contributions to the same antiviral CD8$^+$ T cell response. We discriminated between effects on the primary response, memory formation, and secondary expansion. We found, unexpectedly, that formation of the same CD8$^+$ memory T cell pool, as well as its capacity for secondary expansion, depended on the collective, nonredundant contributions of CD27, 4-1BB, and OX40. In addition, we revealed that 4-1BB and OX40 endowed CD8$^+$ T cells with the capacity for secondary expansion during the primary response.

Materials and Methods

Mice

Wild-type, CD27$^{-/-}$ (25), 4-1BBL$^{-/-}$ (27), and OX40L$^{-/-}$ (31) mice were on C57BL/6 background and used for experiments at 6–10 wk of age, in accordance with institutional and national guidelines. Mice were of the CD45.2 allotype, unless specified otherwise.

Flow cytometry

Lungs, spleens, and lung draining lymph nodes (DLN)[3] were forced through a nylon mesh in IMDM with 8% FCS to acquire single cell suspensions. Erythrocytes were lysed on ice for 2 min in 0.14 M NH_4Cl, 0.017 M Tris-HCl, pH 7.2. Cells were preincubated with Fc block (mAb to CD16/CD32, 2.4G2; BD Biosciences) and washed in staining buffer (PBS, 0.5% BSA, 0.01% sodium azide). Next, cells were incubated with specific Abs conjugated to FITC, PE, or allophycocyanin. Allophycocyanin-labeled tetramers of the murine MHC class I H-2D^b H chain, β_2-microglobulin, and the influenza nuclear protein $(NP)_{366-374}$ peptide ASNENMDAM were prepared as described and used in combination with anti-CD8 mAb (37). Cells were analyzed using a FACSCalibur and CellQuest software (BD Biosciences). Propidium iodide-stained dead cells were excluded from analysis. mAb used for immunofluorescence were anti-CD3ϵ, 500A2; anti-CD8b.2, 53-5.8; anti-CD4, GK1.5; anti-CD11c, N-418; anti-CD27, LG.3A10; anti-CD45R/B220, RA3-6B2; anti-CD45.1, A20; anti-OX40, OX-86; anti-4-1BB, 1AH2 (subclone of 53A2); anti-CD70, 3B9; anti-OX40L, RM134L; and anti-4-1BBL, TKS-1.

Virus infection

Influenza virus strain A/NT/60/68 was grown, purified, and tested for hemagglutinin activity and infectious titers in the Department of Virology, Erasmus University Rotterdam. Mice were anesthetized and infected intranasally with 50 μl of HBSS containing 25 hemagglutinin units of virus to induce primary responses. Six weeks later, 100 hemagglutinin units of the same virus were used to induce memory responses. In this model of viral infection of C57BL/6 mice, we can only read out the CD8$^+$ T cell response with the aid of MHC tetramers, because the immunodominant epitope for CD4$^+$ T cells is undefined.

Determination of virus-specific Ig levels and virus-neutralizing activity

Virus-specific Ig levels were determined, as described previously (38). In brief, blood was collected from the tail vein in heparin-treated tubes. Density gradient-purified influenza virus was coated onto 96-well flat-bottom microtiter plates (Nunc). Wells were incubated with serially diluted sera, followed by biotinylated goat anti-mouse IgM, IgG1, IgG2a, IgG2b, or IgG3 mAb (Southern Biotechnology Associates) and streptavidin-conjugated HRP (Sigma-Aldrich). Substrate 3,3′,5,5′ tetramethylbenzidine (Merck) was used to develop the reaction. Endpoint titers were expressed as reciprocal $\log_3$ of the last dilution, which gave an OD_{450} of $\geq$0.1 OD unit above the OD_{450} of the negative control (pooled serum from nonimmunized mice). Virus-neutralizing activity of serum Ig was tested with the hemagglutination inhibition assay. In this assay, serial serum dilutions are incubated with a standard dose of influenza virus and chicken RBC.

Determination of viral loads

Lungs were harvested at the indicated days after infection and homogenized at 4°C in sterile saline with a tissue homogenizer (BioSpec Products). Lung homogenate was dissolved in TRIzol reagent, and RNA was isolated according to the manufacturer's protocol (Invitrogen Life Technologies). cDNA synthesis was performed using a random hexamer cDNA synthesis kit (Applera). cDNA samples were assayed in duplicate in a 25-μl reaction mixture containing 5 μl of cDNA, 12.5 μl of 2× Taqman Universal PCR Master Mix (Applied Biosystems), 900 nM influenza virus A forward primer (AAG ACC AAT CCT GTC ACC TCT GA), 900 nM influenza virus A reverse primer (CAA AGC GTC TAC GCT GCA GTC C), and 200 nM influenza A probe (TTT GTG TTC ACG CTC ACC GT) (39). The fluorogenic probe was labeled with a 5′ reporter dye, FAM and with a 3′ quencher dye, TAMRA. Amplification and detection were performed in the ABI Prism 7700 sequence-detection system (Applied Biosystems), using the following conditions: 2 min at 50°C and 10 min at 95°C, followed by 45 cycles of 15 s at 95°C and 1 min at 60°C. The viral load present in a sample was calculated using a standard curve of influenza virus in every assay run. Differences between groups were analyzed by a Mann-Whitney *U* test using GraphPad Prism version 4.00 for Windows (GraphPad).

Preparation of purified T cells

Cell suspensions were passed over nylon wool (Polysciences) and incubated on ice for 30 min with mAb M5/114.15.2 to MHC class II (BD Biosciences), followed by 30 min of incubation on ice with 100 μl of goat anti-mouse Ig-coated magnetic beads and 20 μl of sheep anti-rat Ig-coated magnetic beads (Advanced Magnetics) per 10^7 cells. Beads were removed by magnetic sorting.

Adoptive transfers

For all adoptive transfers, purified splenic T cells were used. Where indicated, donor T cells were labeled with CFSE (Molecular Probes) before adoptive transfer (4). Donor T cells were suspended in 200 μl of HBSS and injected into the tail vein of recipient mice at the indicated concentrations, and mice were infected 2 days later. Recipient mice had been infected 6 wk earlier to ensure a primed environment for transferred T cells. For the experiment depicted in Fig. 5, purified T cells isolated from four primed

CD45.2$^+$ wild-type, CD27$^{-/-}$, OX40L$^{-/-}$, and 4-1BBL$^{-/-}$ mice were pooled and stained with H-2D^b/NP$_{366-374}$ tetramers. T cell populations used for adoptive transfer were standardized to contain 1×10^5 H-2D^b/NP$_{366-374}$-specific T cells per CD45.1$^+$ wild-type recipient mouse ($n = 4$). For the experiment depicted in Fig. 6, donor T cells were derived from three primed CD45.1$^+$ wild-type mice, pooled, and injected at 10×10^6 per mouse into CD45.2$^+$ recipient mice of wild-type, OX40L$^{-/-}$, or 4-1BBL$^{-/-}$ phenotype ($n = 3$). For the experiment depicted in Fig. 7, 25×10^6 purified T cells from four naive CD45.1$^+$ mice were first injected into CD45.2$^+$ wild-type, OX40L$^{-/-}$, or 4-1BBL$^{-/-}$ mice, which were infected 2 days later ($n = 3$). After 6 wk, T cells were purified from spleen, pooled, and stained with H-2D^b/NP$_{366-374}$ tetramers as well as with CD45.2-specific mAb. Populations of purified T cells standardized to contain 0.5×10^5 H-2D^b/NP$_{366-374}$-specific T cells of CD45.1$^+$ or CD45.2$^+$ phenotype were injected per wild-type recipient mouse of the CD45.2$^+$ or CD45.1$^+$ phenotype, respectively ($n = 3$).

Results

Primary T cell responses to influenza virus in the absence of CD27, 4-1BBL, and OX40L

Intranasal challenge with influenza virus A/NT/60/68 results in T cell priming in mediastinal lung DLN, followed by an influx of effector T cells into the lung (37). The infection with this strain is mild and not accompanied by extensive lung inflammation or formation of BALT. Among different influenza virus strains tested, A/NT/60/68 best reveals the CD27-deficient phenotype (our unpublished results). To follow virus-specific CD8$^+$ T cells, we used MHC H-2D^b tetramers loaded with the immunodominant NP$_{366-374}$ peptide. In wild-type mice, H-2D^b/NP$_{366-374}$$^+$ CD8$^+$ T cells appeared in the lung at day 6 after infection, reached peak numbers at day 8–10, and declined thereafter (Fig. 1). In the lungs of CD27$^{-/-}$ mice, accumulation of H-2D^b/NP$_{366-374}$-specific T cells was greatly reduced, as documented previously (4, 25). In absence of 4-1BBL, the CD8$^+$ T cell response in lung was also reduced, but to a lesser extent. Similar observations were made for generation of the virus-specific CD8$^+$ T cell pool in DLN: both CD27 and 4-1BB made a contribution, with CD27 having the greatest effect. In contrast, OX40L deficiency did not affect the accumulation of CD8$^+$ virus-specific T cells in either lung or DLN. In the spleen, none of the receptor/ligand systems made a significant contribution to the accumulation of virus-specific CD8$^+$ T cells.

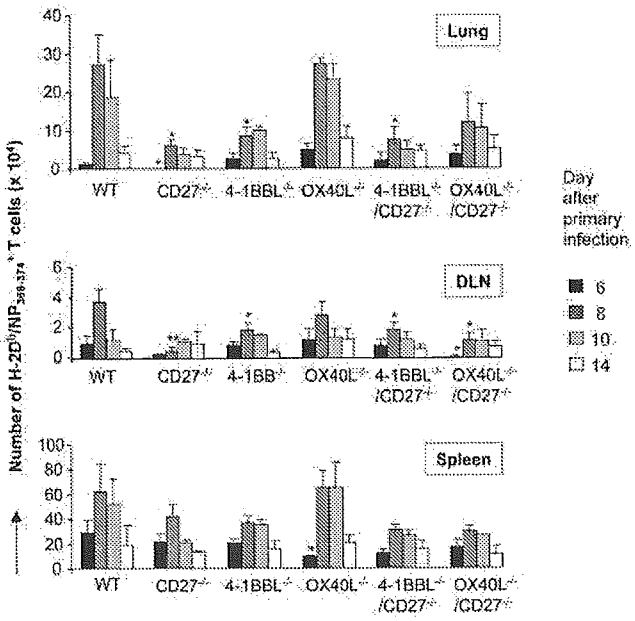

FIGURE 1. Primary CD8$^+$ T cell responses in absence of CD27, 4-1BB, and/or OX40 signals. Wild-type (WT) and recombinant mice were infected with influenza virus. At the indicated days after infection, cells were isolated from lungs, DLN, and spleens; counted; stained with anti-CD8 mAb and H-2D^b/NP$_{366-374}$ tetramers; and analyzed by flow cytometry. Bars represent mean values ($n = 4$); error bars indicate SEM. Two-tailed Student's t test indicated significant differences compared with wild-type values for $p \leq 0.05$ (*) and $p \leq 0.01$ (**). The experiments are representative of two.

To assess a possible redundancy among CD27, 4-1BB, and/or OX40 in establishing the size of the virus-specific CD8$^+$ T cell pool, we also analyzed responses in 4-1BBL/CD27$^{-/-}$ and OX40L/CD27$^{-/-}$ double-deficient mice (Fig. 1). In DLN and lung, additional 4-1BBL or OX40L deficiency did not exacerbate the phenotype of CD27-deficient mice. In addition, redundancy between CD27 and 4-1BB or OX40 did not explain why virus-specific CD8$^+$ T cell accumulation in the spleen was hardly affected in single-deficient mice, because in double-deficient mice no statistically significant reductions in cell accumulation were observed either.

We conclude that upon primary intranasal infection with influenza virus, CD27 makes the most important contribution to generation of virus-specific CD8$^+$ T cells in DLN and their accumulation at the site of infection. 4-1BB also contributes, but to a lesser extent, while OX40 does not. The function of CD27 is nonredundant with that of 4-1BB or OX40. In the spleen, primed CD8$^+$ T cells appear not critically dependent on any of these receptor systems for their accumulation.

Ab responses are not affected in absence of CD27 and 4-1BBL or OX40L

We have shown previously that infection with A/NT60/68 influenza virus results in virus-specific IgG production, which reaches plateau levels between day 14 and 21 after challenge. These Ig levels persist long-term and are only marginally incremented upon renewed challenge with the same virus. The absence of CD27 did not affect Ig production, but only delayed germinal center formation (38). In mice, single deficient for CD27, 4-1BBL, or OX40L, IgM, IgG1, IgG2a, IgG2b, and IgG3 responses were unaltered as compared with responses in wild-type mice (results not shown). Even in mice double deficient for CD27 and 4-1BBL or CD27 and OX40L, these responses proceeded normally and plateau IgG levels attained were similar in all mouse strains (Fig. 2*A*). Also at the peak of the secondary T cell response, IgG titers were not significantly altered in double-deficient mice as compared with those in wild-type mice (Fig. 2*A*). We conclude that the contribution of CD27, 4-1BB, or OX40 is not required for virus-specific IgG production in this model system. Redundancy between CD27 and 4-1BB or OX40 does not explain the lack of effect.

Virus-neutralizing activity of serum Ig was assessed at day 21 after infection by hemagglutination inhibition assay and found to be comparable in wild-type, 4-1BBL/CD27$^{-/-}$, and OX40L/CD27$^{-/-}$ mice. Viral load was determined by PCR in total lung extracts of wild-type, 4-1BBL/CD27$^{-/-}$, and OX40L/CD27$^{-/-}$ mice at days 4, 7, 14, and 21 after primary infection (Fig. 2*B*). In agreement with the unaltered IgG response in the different recombinant strains and the lack of effect of CD27 and 4-1BBL or OX40L deletion on the virus-neutralizing activity of serum Ig, we found that clearing of influenza virus from the lungs of wild type and double deficient proceeded with similar kinetics and efficacy. Viral load peaked at or before day 4 after infection, and virus was cleared by day 21. The only statistically significant difference ($p < 0.05$) was for OX40L/CD27$^{-/-}$ mice vs wild-type and 4-1BBL$^{-/-}$ mice at day 7.

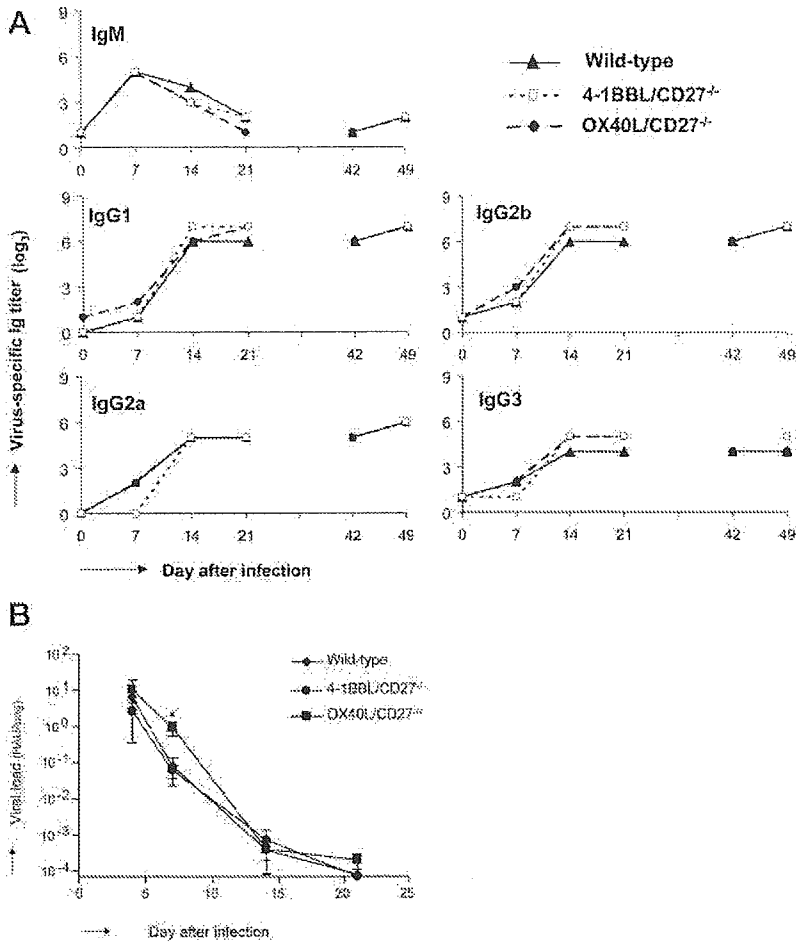

FIGURE 2. Ig responses and viral load in absence of CD27, 4-1BB, and/or OX40 signals. *A*, At the indicated days after infection, serum titers of the indicated virus-specific Ig isotypes in wild-type, 4-1BBL/CD27$^{-/-}$, and OX40L/CD27$^{-/-}$ mice were determined by ELISA. Primary challenge was done at day 0, and secondary challenge at day 42. Each data point represents a measurement on pooled sera from five mice. Titers are expressed as outlined in *Materials and Methods*. *B*, Viral load in lungs of the indicated mice at days 4, 7, 14, and 21 after infection was determined by PCR. It is presented as means + SE in hemagglutinating units per lung. The limit of detection is at 6.95×10^{-5} hemagglutinating units/lung. Data are derived from three to four mice per group.

Memory T cell responses to influenza virus in the absence of CD27, 4-1BBL, and OX40L

To compare the capacity of mice deficient for CD27, 4-1BBL, or OX40L to mount a memory CD8$^+$ T cell response, mice were reinfected with the same virus 6 wk after the first challenge. The occurrence of H-2D^b/NP$_{366-374}$$^+$ CD8$^+$ T cells was determined 3, 5, 7, and 11 days after secondary infection. Characteristically, H-2D^b/NP$_{366-374}$$^+$-specific T cells reached peak levels earlier in lungs of wild-type mice earlier than in the primary response (day 5 vs days 8–10) and were higher in number (Fig. 3). Strikingly, in this secondary response, all three receptor/ligand systems were required for accumulation of H-2D^b/NP$_{366-374}$$^+$-specific T cells in the lung. In DLN and spleen, generation of H-2D^b/NP$_{366-374}$$^+$ memory effector T cells was also reduced. CD27 deficiency had the most profound impact, while lack of 4-1BBL had some effect and lack of OX40L had almost no statistically significant consequences (Fig. 3).

Analysis of responses in 4-1BBL/CD27$^{-/-}$ and OX40L/CD27$^{-/-}$ double-deficient mice revealed complementarity between CD27 and 4-1BB or OX40. In lung, and particularly in DLN and spleen, accumulation of virus-specific CD8$^+$ T cells was further reduced in double-deficient mice than in single-deficient mice (Fig. 3). These data demonstrate that the memory CD8$^+$ T cell response to intranasal infection with influenza virus critically depends on the collective, partially nonredundant contributions that result from interaction among CD27, 4-1BB, OX40, and their ligands.

Formation of memory CD8$^+$ T cells in the absence of CD27, 4-1BBL, and OX40L

Accumulation of effector T cells in the memory response is determined by two key parameters: the number of memory T cells formed and the extent of their secondary expansion. To better understand the effect of CD27, 4-1BB, and OX40 on accumulation of virus-specific T cells in the memory response, we studied their impact on these parameters separately. First, we determined the effect of CD27, 4-1BBL, or OX40L deficiency on the generation of memory CD8$^+$ T cells. In blood of wild-type mice, the percentage of T cells within the CD8$^+$ population that stained with H-2D^b/NP$_{366-374}$ tetramers at 6 wk after primary infection was >7-fold higher than in naive mice, indicating the presence of memory (Fig. 4*A*). In mice deficient for CD27, 4-1BBL, or OX40L, CD8$^+$ memory T cell levels were almost 2-fold reduced as compared with wild type, while in 4-1BBL/CD27$^{-/-}$ and OX40L/CD27$^{-/-}$ mice these numbers were a further 2-fold reduced, coming close to background levels in naive mice (Fig. 4*A*). In spleens of wild-type memory mice, H-2D^b/NP$_{366-374}$$^+$ T cell numbers were increased ~6-fold as compared with numbers found in naive mice. In CD27$^{-/-}$, 4-1BBL$^{-/-}$, and OX40L$^{-/-}$ mice, levels of H-2D^b/NP$_{366-374}$-specific memory T cells were reduced ~2-fold as compared with those in wild-type mice (Fig. 4*B*). Interestingly, in the lungs of previously infected mice, numbers of tetramer$^+$ T cells were ~10-fold higher than in naive mice. These most likely represent tissue memory cells, because their adoptive transfer gave rise to a memory response (results not shown). As in the spleen, all

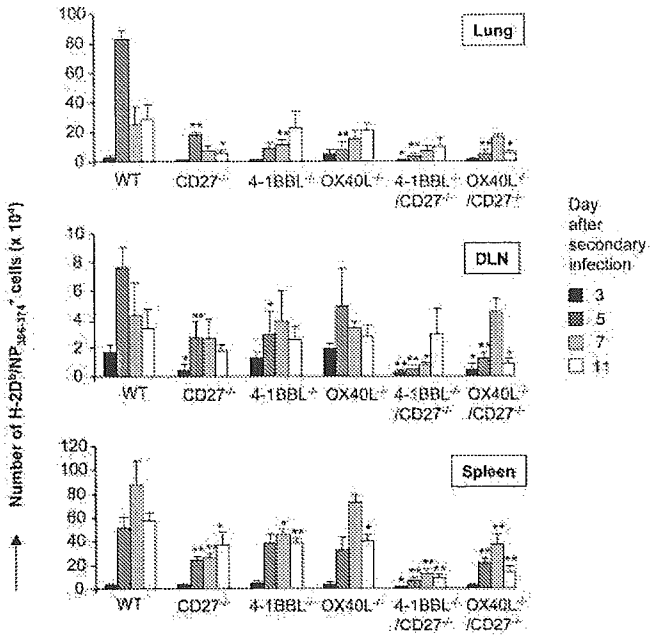

FIGURE 3. Memory $CD8^+$ T cell responses in absence of CD27, 4-1BB, and/or OX40 signals. Six weeks after primary infection, mice of the indicated genotypes were reinfected with the same influenza virus strain. Cells were analyzed as outlined for Fig. 1. Bars represent mean values (n = 4); error bars indicate SEM. Two-tailed Student's t test indicated significant differences compared with wild-type values for $p \leq 0.05$ (*) and $p \leq 0.01$ (**). The experiments are representative of two.

three receptor/ligand systems promoted memory T cell formation in the lung, with CD27/CD70 and 4-1BB/4-1BBL having a greater effect than OX40/OX40L (Fig. 4*B*).

We conclude that after intranasal influenza virus infection, generation of the $CD8^+$ central and tissue memory T cell pools relies on collective, nonredundant contributions of CD27, 4-1BB, and OX40. Although OX40L deficiency did not affect the accumulation of virus-specific $CD8^+$ T cells in the primary response, it did reduce memory T cell formation. This suggests that OX40/OX40L interactions promote T cell survival in the contraction and/or memory phase. Interaction between CD27, 4-1BB, and their ligands may similarly do so and may in addition promote memory $CD8^+$ T cell formation by incrementing the size of the $CD8^+$ effector T cell pool.

Secondary expansion of memory T cells from CD27$^{-/-}$, 4-1BBL$^{-/-}$, or OX40L$^{-/-}$ mice

To determine the contribution of CD27, 4-1BBL, and OX40L to expansion and accumulation of memory $CD8^+$ T cells during the secondary response, we performed adoptive transfer experiments. A small sample of the T cells that were purified from spleens of primed wild-type, $CD27^{-/-}$, $4\text{-}1BBL^{-/-}$, and $OX40L^{-/-}$ was set aside and stained with tetramers. This allowed adjustment of the number of cells used for adoptive transfer, so that each recipient mouse received an equal amount of $H\text{-}2D^b/NP_{366-374}$-specific T cells (see Fig. 4 for numbers of memory cells in this experiment). In this way, we corrected for the effects of CD27, 4-1BBL, and OX40L deficiency on memory T cell formation, allowing us to monitor their effect on secondary expansion as such. Donor T cells were labeled with CFSE and injected into primed wild-type recipient mice. Their accumulation was analyzed at day 6 after secondary infection (Fig. 5*A*).

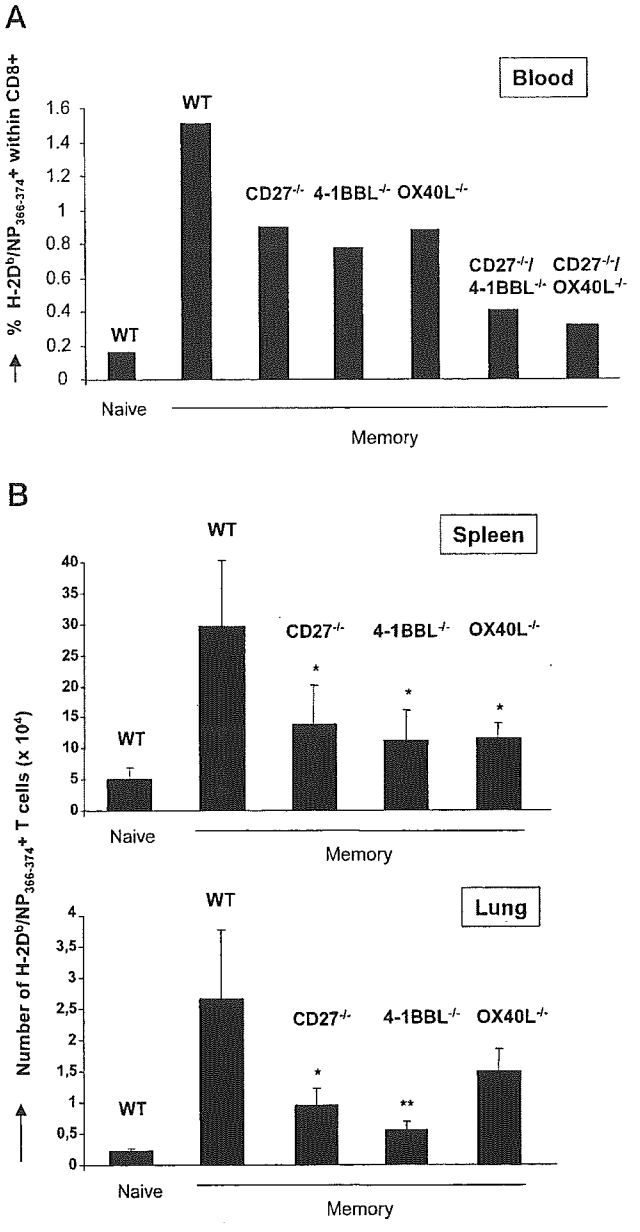

FIGURE 4. Formation of $CD8^+$ T cell memory in absence of CD27, 4-1BB, and/or OX40 signals. *A*, Blood was collected from wild-type (WT) and recombinant mice at 6 wk after infection, as well as from naive WT mice (n = 6, pooled). Bars represent percentage of $tetramer^+$ cells within the $CD8^+$ population. *B*, Cells were harvested from spleens and lungs of WT, $CD27^{-/-}$, $4\text{-}1BBL^{-/-}$, and $OX40L^{-/-}$ mice at 6 wk after influenza infection (n = 4). Bars represent mean number of $tetramer^+$ $CD8^+$ T cells. Results are representative of two experiments.

In spleen, lung, and DLN, accumulation of $H\text{-}2D^b/NP_{366-374}$-specific T cells derived from primed $CD27^{-/-}$, $4\text{-}1BBL^{-/-}$, or $OX40L^{-/-}$ mice was significantly reduced as compared with accumulation of T cells from primed wild-type mice (Fig. 5*B*). The total pool of responding $CD8^+$ T cells (based on CFSE loss) was also significantly decreased in case memory T cells were derived from CD27-, 4-1BBL-, or OX40L-deficient mice. This was particularly clear in lung, but could also be observed in the spleen. In DLN, only OX40L deficiency had a significant effect on the total $CD8^+$ responder pool. We do not know to which extent the total $CD8^+$ responder T cell pool represents bystander cells, but it very

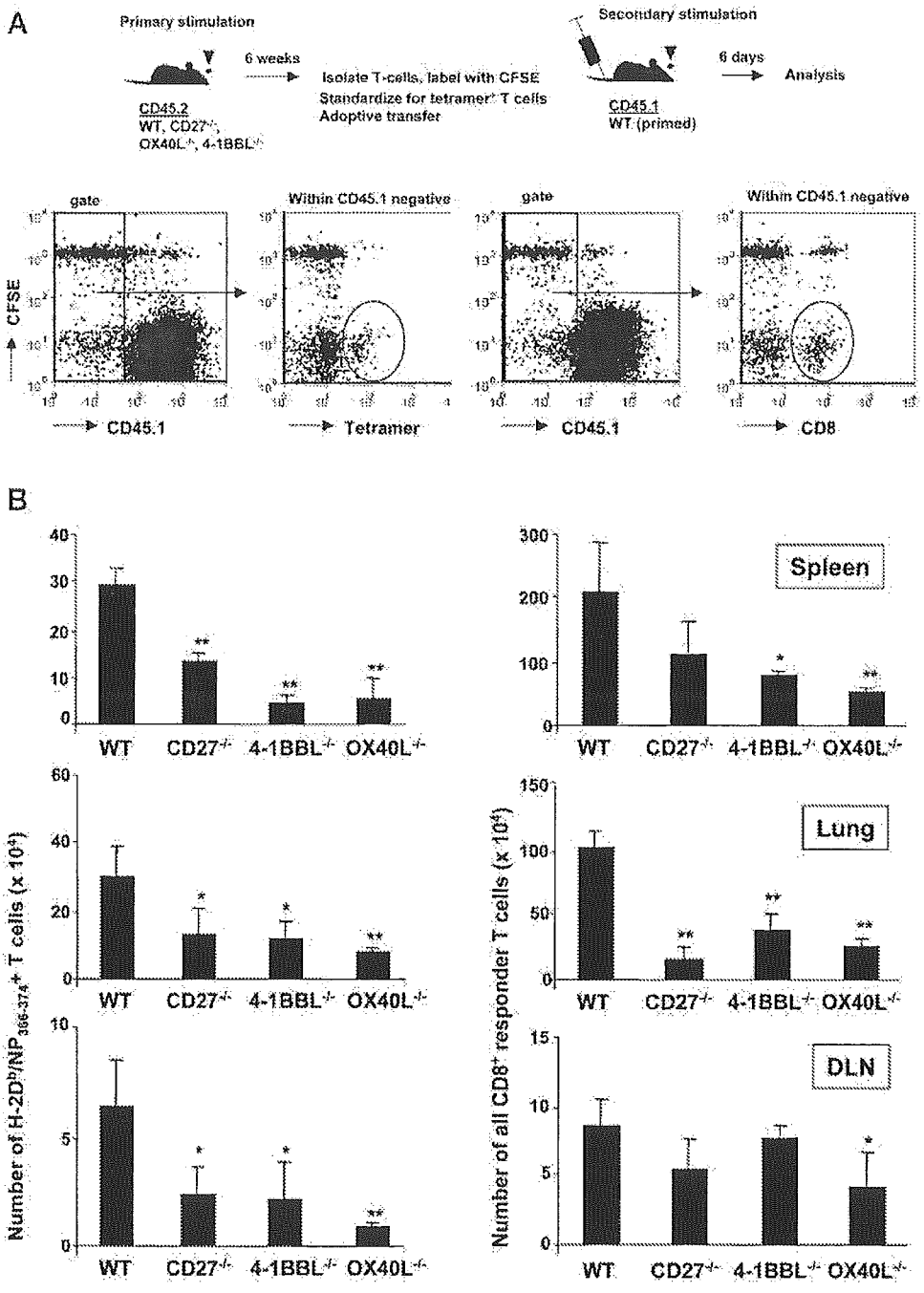

FIGURE 5. Secondary expansion of CD8$^+$ memory T cells from CD27$^{-/-}$, 4-1BBL$^{-/-}$, or OX40L$^{-/-}$ mice in wild-type recipients. *A*, Experimental setup. Wild-type (WT), CD27$^{-/-}$, 4-1BBL$^{-/-}$, and OX40L$^{-/-}$ mice of the CD45.2 allotype were infected with influenza virus. After 6 wk, T cells were purified from spleen, stained with H-2D^b/NP$_{366-374}$ tetramers and anti-CD8 mAb, and labeled with CFSE. T cell samples, standardized to contain equal numbers of tetramer$^+$ T cells, were injected into primed CD45.1$^+$ wild type. At day 6 after secondary infection, cells from spleens, lungs, and DLN were stained with anti-CD45.1 mAb, NP$_{366-374}$/H-2D^b tetramers, and anti-CD8 mAb, and analyzed by flow cytometry. Representative dot plots of WT spleen samples show gating on donor cells and the definition of responder cell by CFSE dilution in tetramer$^+$ and total CD8$^+$ populations. *B*, Absolute numbers of either tetramer$^+$ or CD8$^+$ responder T cells from the donor, calculated from the percentage of tetramer$^+$/CD45.1$^-$/CFSE$^-$ or CD8$^+$/CD45.1$^-$/CFSE$^-$ cells and the total number of cells per organ. Bars represent means (n = 4). The experiment shown is representative of two.

likely includes virus-specific T cells, because influenza virus contains other immunogenic MHC class I-restricted epitopes besides NP$_{366-374}$ (40). We conclude that memory CD8$^+$ T cells specific for the H-2D^b/NP$_{366-374}$ complex, as well as memory CD8$^+$ T cells with other virus specificities, are dependent on the collective contributions of CD27, 4-1BBL, and OX40L for their secondary expansion and establishment at the site of infection.

Memory CD8$^+$ T cells do not require support by 4-1BBL and OX40L on non-T cells throughout the secondary response

In the experiment described above, memory T cells derived from 4-1BBL$^{-/-}$ or OX40L$^{-/-}$ mice normally expressed 4-1BB or OX40, while their ligands were present in the wild-type recipients. We considered therefore that absence of 4-1BBL or OX40L during the primary response might have compromised the intrinsic capacity of memory T cells from 4-1BBL$^{-/-}$ and OX40L$^{-/-}$ mice to expand upon renewed challenge. Subsequent experiments were designed to address this possibility.

To test whether 4-1BBL or OX40L was required throughout the secondary response, we examined secondary expansion of wild-type memory cells in a ligand-deficient environment. T cells were purified from the spleen of primed wild-type mice, labeled with CFSE, and allowed to undergo secondary expansion in wild-type, 4-1BBL$^{-/-}$, or OX40L$^{-/-}$ recipients. The response was analyzed as outlined for Fig. 5. It appeared that wild-type memory CD8$^+$ T cells expanded and accumulated in spleen, lung, and DLN of 4-1BBL$^{-/-}$ or OX40L$^{-/-}$ recipients to a similar extent as in wild-type recipients (Fig. 6). Both H-2D^b/NP$_{366-374}$-specific and total CD8$^+$ memory T cells were independent of 4-1BBL or OX40L for their accumulation. In this system, the only cells that may express 4-1BBL or OX40L are the transferred T cells themselves. We conclude, therefore, that memory CD8$^+$ T cells do not require

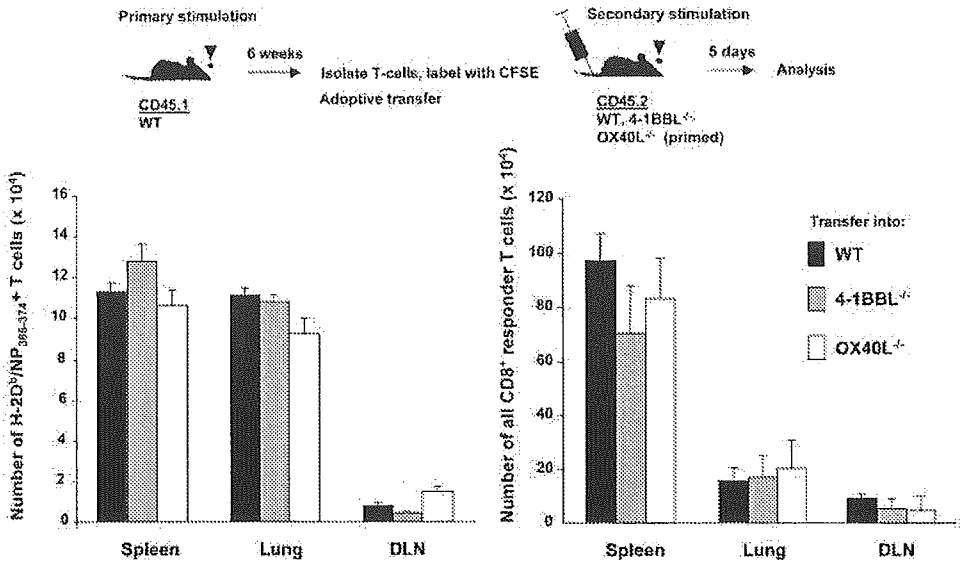

FIGURE 6. Secondary expansion of wild-type memory $CD8^+$ T cells in 4-1BBL$^{-/-}$ or OX40L$^{-/-}$ recipients. Wild-type (WT) CD45.1$^+$ mice were infected with influenza virus. Six weeks later, T cells were isolated from spleen, labeled with CFSE, and injected into primed CD45.2$^+$ WT, 4-1BBL$^{-/-}$, or OX40L$^{-/-}$ recipients. At day 5 after secondary infection, cells from spleens, lungs, and DLN were stained with anti-CD45.1 mAb, H-2D^b/$NP_{366-374}$ tetramers, and anti-CD8 mAb, and analyzed by flow cytometry. Absolute numbers of either tetramer$^+$ or $CD8^+$ responder T cells were calculated from the percentage of tetramer$^+$/CD45.1$^+$/CFSE$^-$ or $CD8^+$/CD45.1$^+$/CFSE$^-$ cells and the total number of cells per organ. Bars represent means (n = 3). The experiment shown is representative of two.

expression of 4-1BBL or OX40L on non-T cells throughout the secondary response for their expansion in spleen and DLN and for their accumulation in lung, the site of infection.

4-1BBL and OX40L on non-T cells imprint the capacity for secondary expansion in $CD8^+$ T cells during the primary response

The finding that wild-type memory T cells could expand well in 4-1BBL$^{-/-}$ or OX40L$^{-/-}$ recipients suggested that either ligands on the memory T cells themselves supported secondary expansion, or that the potential for secondary expansion was imprinted into T cells by receptor/ligand interactions that occurred during the primary response. To address these possibilities, we primed wild-type T cells in 4-1BBL$^{-/-}$ or OX40L$^{-/-}$ recipients, monitored their conversion to $CD8^+$ memory T cells, and subsequently let standardized numbers of memory cells respond to rechallenge in wild-type mice. In this experiment, we also tested the capacity of $CD8^+$ T cells from the 4-1BBL$^{-/-}$ and OX40L$^{-/-}$ recipients to form memory and to respond to rechallenge in wild-type mice (Fig. 7*A*).

The capacity of wild-type $CD8^+$ T cells to form memory in 4-1BBL$^{-/-}$ or OX40L$^{-/-}$ recipients (as monitored in blood) was reduced as compared with the wild-type situation (Fig. 7*B*). In fact, wild-type $CD8^+$ T cells formed H-2D^b/$NP_{366-374}$-specific memory in 4-1BBL$^{-/-}$ or OX40L$^{-/-}$ recipients as inadequately as $CD8^+$ T cells from these recipients themselves. Apparently, $CD8^+$ T cells require stimulation of 4-1BB and OX40 by their ligands on non-T cells for memory formation.

As also shown in Fig. 5*B*, the secondary response of H-2D^b/$NP_{366-374}$-specific memory T cells, as well as total $CD8^+$ T cells from 4-1BBL$^{-/-}$ or OX40L$^{-/-}$ first recipients in wild-type secondary recipients was impaired, as evident from their significantly decreased accumulation in spleen, DLN, and lung (Fig. 7*C*). Interestingly, wild-type $CD8^+$ memory T cells primed in a 4-1BBL$^{-/-}$ or OX40L$^{-/-}$ environment were also impaired in secondary responsiveness (Fig. 7*D*). This was evident from the significantly reduced expansion of H-2D^b/$NP_{366-374}$-specific T cells in the spleen and their reduced accumulation in the lung. The defect in the lung was also statistically significant for the total $CD8^+$ T cell population (Fig. 7*D*). From this experiment, we derive the conclusion that triggering of 4-1BB or OX40 by their ligands on non-T cells during the primary response imprints into memory $CD8^+$ T cells the potential to efficiently expand and accumulate upon secondary challenge. The fact that secondary expansion of memory T cells from ligand-deficient mice was more severely affected than that of memory T cells from wild-type mice (Fig. 7, compare *C* and *D*) can be explained by a contribution of ligand on T cells to imprinting for secondary expansion and/or by undefined intrinsic differences between T cells of wild-type and ligand-deficient genotype.

Expression of receptors and ligands on T cells and APCs during antiviral responses

To understand where and when throughout the immune response to influenza virus CD27, 4-1BB, OX40, and their ligands might interact, we performed an extensive analysis of their expression. At different time points after infection, cells were isolated from lung, DLN, and spleen and double stained with Ab to the relevant receptor or ligand and to CD3 as T cell marker, CD19 as B cell marker, or CD11c as marker for myeloid cells, in particular DC. The expression of receptors and ligands was consistently most pronounced in the lung (Fig. 8), as compared with DLN and spleen (data not shown). With regard to the receptors, we found that CD27 was clearly expressed on the great majority of T cells in DLN, spleen, and lung throughout primary and memory responses (Fig. 8*A*). On the days examined, 4-1BB was virtually undetectable on T cells, but quite prominent on $CD11c^+$ cells in lung (Fig. 8*A*), DLN, and spleen (data not shown). OX40 was found on a minority of T cells, which were most abundant in the lung during the primary response (Fig. 8*A*). CD27 and OX40 were also present on $CD11c^+$ cells in these organs, but to a lesser extent than 4-1BB (Fig. 8*A*, and results not shown). Expression of the receptors on B cells was generally of low intensity and frequency, although 4-1BB was clearly detectable on B cells in the lung during the primary response (Fig. 8*A*).

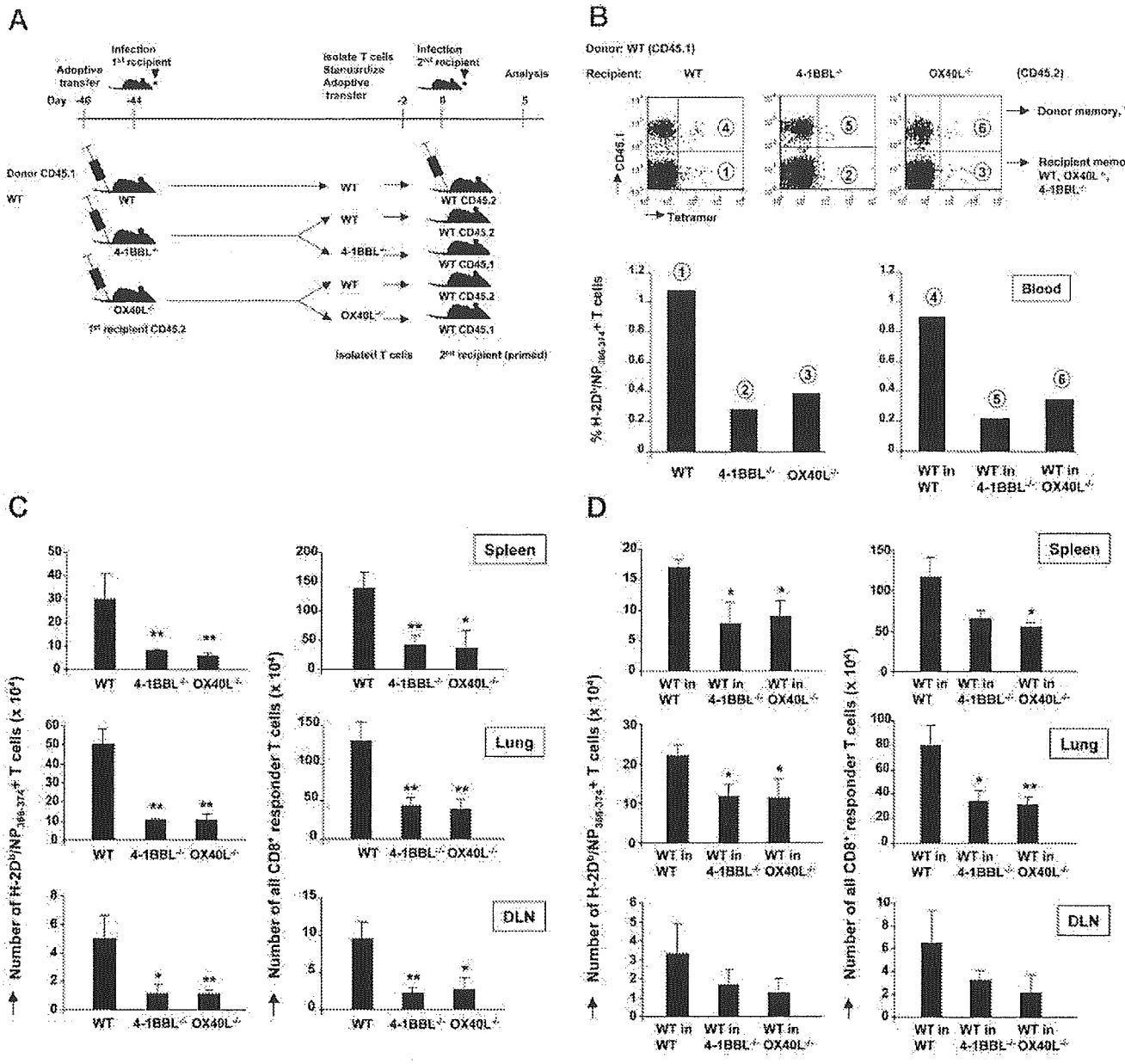

FIGURE 7. Wild-type T cells primed in absence of 4-1BBL or OX40L show defective secondary expansion. *A*, Experimental design. Purified splenic T cells from naive wild-type (WT) CD45.1$^+$ mice were injected into naive CD45.2$^+$ wild-type, 4-1BBL$^{-/-}$, or OX40L$^{-/-}$ mice. At 6 wk after infection, T cells were purified from spleen and stained with anti-CD45.1 mAb; H-2D^b/NP$_{366-374}$ tetramers and anti-CD8 mAb to determine memory T cell formation. Next, populations of purified splenic T cells, standardized for numbers of tetramer$^+$ T cells, were injected into primed WT secondary recipients. CD45.1$^+$ T cells from the primary WT donors were injected into CD45.2$^+$ recipients and CD45.2$^+$ T cells from WT, 4-1BBL$^{-/-}$, or OX40L$^{-/-}$ first recipients into CD45.1$^+$ second recipients. *B*, Dot plots show CD45.1$^+$ donor-derived and CD45.1$^-$ (CD45.2$^+$) recipient-derived memory T cell populations with H-2D^b/NP$_{366-374}$ specificity in blood, as detected 6 wk after infection of the first recipients. Bars indicate percentage of tetramer$^+$ cells (n = 3, pooled). *C* and *D*, At day 5 after secondary infection, cells from spleens, lungs, and DLN were stained with anti-CD45.1 mAb, tetramers, and anti-CD8 mAb, and analyzed by flow cytometry. Absolute numbers of either tetramer$^+$ or CD8$^+$ T cells were calculated, as outlined for Fig. 4. Bars represent means (n = 3). *C*, Shows the result for CD45.2$^+$ T cells of the first recipient (WT, 4-1BBL$^{-/-}$, or OX40L$^{-/-}$); *D*, Shows the results for wild-type CD45.1$^+$ T cells of the primary donor. The experiment shown is representative of two.

The ligands of the TNF family are notoriously difficult to detect because they are transiently expressed, contingent upon immune activation. We found CD70, 4-1BBL, and OX40L on T cells in DLN, spleen, and lung, but at low frequency. The ligands were most prominent on CD11c$^+$ cells, while they were also found on B cells (Fig. 8*B*). From comparing expression of CD27, 4-1BB, OX40, and their ligands in the lung throughout primary and secondary responses, it appears that 4-1BB/4-1BBL and OX40/OX40L are much less prominently expressed in the secondary response (Fig. 8, *A* and *B*).

The primary data in Fig. 8*C* highlight the transient and activation-specific nature of ligand expression, in this case on CD11c$^+$ (DC) in the lung, the site where they were most abundant. Throughout the primary response, the ligands were acquired by CD11c$^+$ cells in the lung and subsequently lost. Cell surface expression of CD70 was at all times very low, making the exact

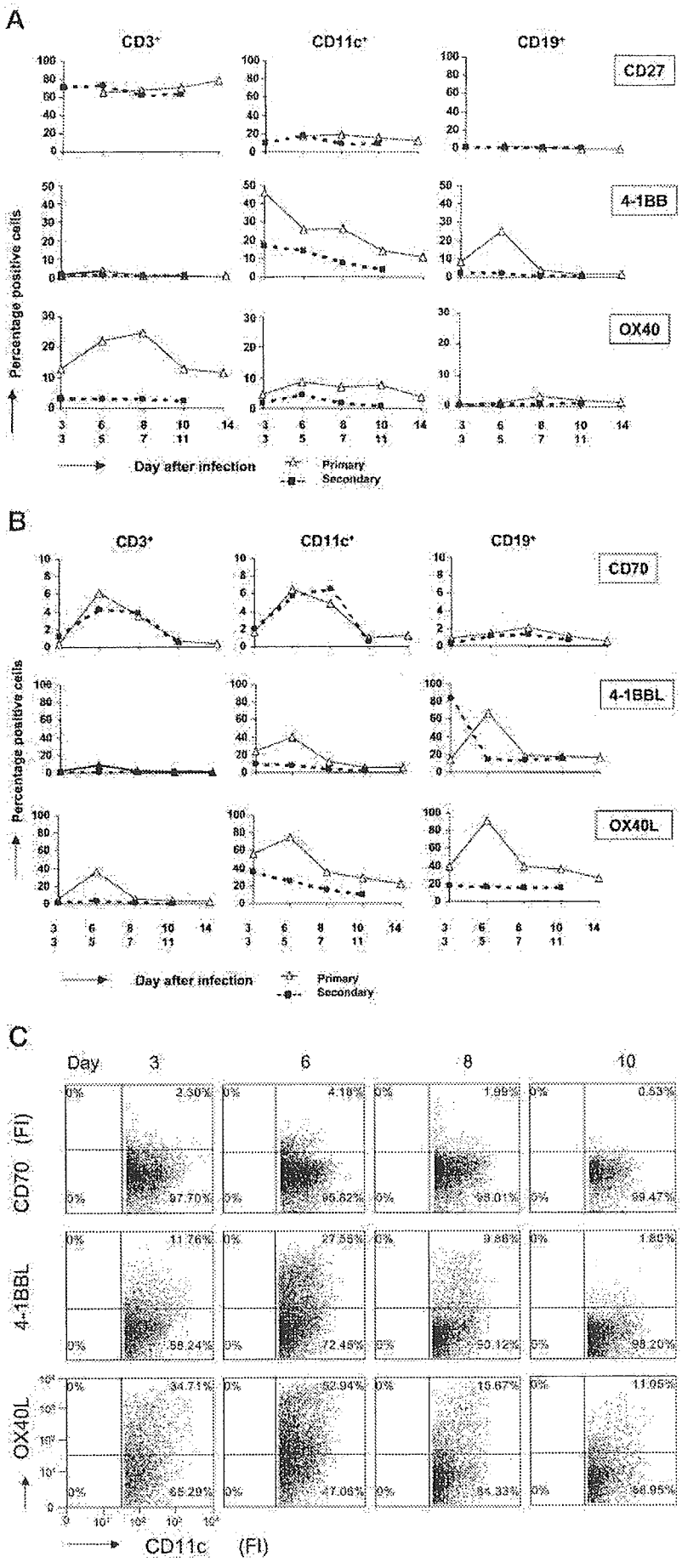

FIGURE 8. Expression of receptors and ligands in lung during primary and secondary infection. At the indicated time points after primary or secondary infection, cells extracted from lungs were stained with Abs for CD3, CD11c, or CD19; combined with Abs for CD27, 4-1BB, OX40, CD70, 4-1BBL, or OX40L; and analyzed by flow cytometry. *A*, Percentage of lung-infiltrating $CD3^+$ cells (T cells), $CD11c^+$ cells (enriched for DC), and $CD19^+$ cells (B cells) expressing CD27, 4-1BB, or OX40. *B*, Percentage of these populations expressing CD70, 4-1BBL, or OX40L. *C*, Flow cytometry dot plots showing fluorescence intensity of CD70, 4-1BBL, and OX40L staining on gated lung-infiltrating $CD11c^+$ cells.

percentage of positive cells difficult to determine. However, 4-1BBL and OX40L were expressed at high levels on large fractions of CD11c$^+$ cells at day 6 after primary infection, a time when effector T cells start entering the lung (Fig. 8*C*). B cells in the lung also express significant levels of these ligands (Fig. 8*B*). These data suggest that CD11c$^+$ cells (DC) and B cells at the effector site may play a role in regulating the size of the effector and memory T cell pools, as well as the functional properties of developing memory cells.

Discussion

In this study, we have determined that upon intranasal infection with influenza virus, CD27, 4-1BB, and OX40 collectively shape the same CD8$^+$ T cell memory pool, both in terms of numbers of memory T cells formed and their capacity to accumulate upon secondary challenge. The contributions of CD27, 4-1BB, and OX40 receptor/ligand systems to T cell responsiveness had not previously been compared side by side in the same model of antigenic challenge. Unexpectedly, we have also revealed that 4-1BB and OX40 endow memory CD8$^+$ T cells during their formation with an improved capacity for secondary responsiveness.

As shown for OX40 receptor deficiency (29), we found that OX40L deficiency did not compromise the primary CD8$^+$ effector T cell response to intranasally delivered influenza virus. OX40-Ig fusion protein was recently shown to reduce both CD4$^+$ and CD8$^+$ T cell numbers in the lungs of mice primed with HKx31 influenza virus, which was the first in vivo evidence that OX40 can promote primary CD8$^+$ T cell responses (33). A recent report monitoring anti-OVA responses of OX40-deficient CD8$^+$ T cells corroborates this (34). In a model of i.p. injection with influenza virus (HKx31), virus-specific CD8$^+$ T cell accumulation in the spleen during the effector phase was normal in mice lacking 4-1BBL, OX40L, or both (28, 35). In our model of intranasal virus delivery, however, 4-1BBL deficiency did reduce generation of the CD8$^+$ effector T cell pool in DLN and its establishment in the lung. Consistent with Bertram et al. (28), we found no contribution of 4-1BB/4-1BBL to the primary T cell response in the spleen. CD27 similarly did not affect the primary CD8$^+$ T cell response in this organ. We suspect that the splenic microenvironment may be different from DLN and lung tissue in that it offers alternative modes of survival support to activated T cells.

We have found that CD27 makes a greater contribution to the primary CD8$^+$ T cell response than 4-1BB/4-1BBL. This can be explained by the fact that CD27 is already expressed on naive T cells and contributes to T cell survival from the moment of priming. Nevertheless, CD27 and 4-1BBL make complementary contributions to the primary response. Possibly, their mechanism of action is the same, but activated T cells may meet CD70 and 4-1BBL at different moments after their initial activation. Alternatively, CD27 and 4-1BB may up-regulate different antiapoptotic molecules, which differ in their capacity to counteract certain death signals that operate in activated T cells. A third possibility is that CD27 and 4-1BB differ in their capacity to direct cellular responses unrelated to apoptosis.

With regard to the formation of memory T cells, it is well established that deliberate ligation of 4-1BB or OX40 prevents clonal deletion of previously activated T cells and enlarges the memory T cell pool in the spleen. In case of OX40, this effect was more profound for CD4$^+$ T cells than for CD8$^+$ T cells, while for 4-1BB it was the other way around (22, 23). After i.p. challenge with influenza virus, 4-1BBL$^{-/-}$ mice showed a reduction in virus-specific CD8$^+$ T cells late in the primary response and upon rechallenge, while OX40L$^{-/-}$ mice had no defects (28, 35). In this study, we show that upon intranasal delivery of influenza virus, 4-1BB, CD27, and OX40 collectively shape the same CD8$^+$ T cell memory T cell pool. In the intranasal influenza virus model, absolute numbers of H-2D^b/NP$_{366-374}$ memory T cells are low, but tetramer staining is manifold over background levels found in naive mice. Moreover, adoptive transfer experiments for spleen and lung corroborated the existence of memory on basis of kinetics and efficiency of the secondary response (our unpublished results). The contributions of CD27, 4-1BBL, and OX40L to T cell memory in the circulation were comparable in magnitude. Given the similarity in viral clearing in wild-type and double-deficient mice, it is unlikely that viral loads have had a major differential impact on memory formation in the wild-type and recombinant strains.

Our data indicate that CD27, 4-1BBL, and OX40L contribute to central as well as tissue memory formation of CD8$^+$ T cells. Interesting in this respect is that expression of CD70, 4-1BBL, and OX40L is most pronounced at the effector site. Unexpectedly, both CD11c$^+$ cells and B cells in the lung carried these ligands. We suggest that communication between effector T cells and APCs (DC, B cells) via these receptor/ligand systems at the tissue site may regulate the size of the effector T cell pool and the extent of effector T cell contraction. The finding that OX40L deficiency did not affect the size of the effector T cell pool, but compromised the size of the memory T cell pool, suggests that it acted during the contraction and/or memory phase. Complementarity between the three receptor/ligand systems seems to lie in part in the timing of their involvement in the primary response. In this scenario, CD27 would be first and OX40 the last to make a prosurvival contribution.

We had difficulty in detecting 4-1BB and OX40 on T cells in vivo, but in vitro studies have proven that these receptors directly transmit survival signals into T cells (6, 7). Therefore, we assume that the effects on T cell responsiveness observed in OX40L- and 4-1BBL-deficient mice are at least in part due to defective signaling via OX40 and 4-1BB into T cells. However, the detection of both receptors and ligands on CD11c$^+$ cells in infected mice has warned us that effects on T cells may also in part be indirect, i.e., proceed via the modulation of DC function. Our novel finding that CD11c$^+$ cells can express both CD70 and CD27 indicates that these may similarly affect T cell function indirectly.

An important aspect of our work is that we have separated effects of CD27, 4-1BB, and OX40 on memory formation from those on secondary expansion. This has been done using T cell populations, which were standardized for the amount of H-2D^b/NP$_{366-374}$-specific cells for adoptive transfer. This setup has allowed us to uncover that memory T cells do not need support by 4-1BBL or OX40L during secondary expansion, but require it for optimal programming during the primary response. One study that has used a similar approach documents normal secondary expansion of primed T cells from 4-1BBL$^{-/-}$ mice in wild-type recipients (41). We believe that the difference may be due to the i.p. challenge with influenza virus that was used. As discussed above, this may involve a mode of priming (in the spleen) that bypasses the need for survival support by 4-1BB and its relatives. Because CD70-deficient mice are not available, we could not use a similar setup to test whether CD27 can imprint into CD8$^+$ T cells the capacity for secondary expansion. However, a recent study using recombinant soluble CD70 for costimulation during primary challenge with OVA suggests that this might be the case (42).

An important subject of recent studies is the question as to whether T cell responses proceed according to a pre-established program after initial Ag encounter. TCR stimulation triggers a developmental program in naive CD8$^+$ T cells, allowing them, in the

subsequent absence of Ag, to divide at least seven times, to develop cytolytic effector functions, and to acquire memory characteristics (43, 44). However, our data argue that Ag is an important factor in controlling T cell survival and the extent of memory formation. We postulate that when Ag wanes, CD70, 4-1BBL, and OX40L disappear and with them the prosurvival effects of their receptors. In such a scenario, Ag does not necessarily control effector and memory cell differentiation, but it does determine the amount of effector and memory cells formed. Presumably, the requirement for continuous input via CD27 and its related receptors into T cells is required to maintain expression of antiapoptotic molecules. In the memory phase, survival support comes from cytokines such as IL-15 (45).

Evidence has been presented recently that $CD4^+$ T cells can program the capacity for secondary expansion into $CD8^+$ T cells during priming (46–48). Whether the effect of 4-1BB and OX40 triggering on memory formation and secondary responsiveness impacts directly on $CD8^+$ T cells or affects these indirectly via $CD4^+$ T cells remains to be shown. However, it is excluded that $CD8^+$ memory formation and responsiveness are exclusively regulated by 4-1BBL or OX40L on $CD4^+$ T cells, because we have proven that ligands on non-T cells are also important for this. We do not know when the programming for secondary expansion occurs, or what it entails at a molecular level. Because memory T cells are slowly cycling (45), it must be a capacity that can be transmitted to the daughter cells and therefore can truly be termed programming. Our collective data strongly support the idea that deliberate offering of CD70, 4-1BBL, and OX40L during priming may be a good strategy to achieve potent and long-lasting immunity.

Acknowledgments

We thank J. J. Peschon (Amgen) for kindly providing 4-$1BBL^{-/-}$ mice; the members of the experimental animal and flow cytometry facilities of The Netherlands Cancer Institute for excellent technical assistance; A. M. van Loon (Department of Virology, University Medical Center) for advice; and T. N. M. Schumacher, K. Schepers, and R. Arens (Division of Immunology, The Netherlands Cancer Institute) for advice and for critically reading the manuscript.

Disclosures

The authors have no financial conflict of interest.

References

1. Watts, T. H., and M. A. DeBenedette. 1999. T cell costimulatory molecules other than CD28. *Curr. Opin. Immunol.* 11: 286–293.
2. Croft, M. 2003. Co-stimulatory members of the TNFR family: keys to effective immunity? *Nat. Rev. Immunol.* 3: 609–619.
3. Gravestein, L. A., and J. Borst. 1998. Tumor necrosis factor receptor family members in the immune system. *Semin. Immunol.* 10: 423–434.
4. Hendriks, J., Y. Xiao, and J. Borst. 2003. CD27 promotes survival of activated T cells and complements CD28 in generation and establishment of the effector T cell pool. *J. Exp. Med.* 198: 1369–1380.
5. Okkenhaug, K., L. Wu, K. M. Garza, J. La Rose, W. Khoo, N. Odermatt, T. W. Mak, P. Ohashi, and R. Rottapel. 2001. A point mutation in CD28 distinguishes proliferative signals from survival signals. *Nat. Immunol.* 2: 325–332.
6. Rogers, P. R., J. Song, I. Gramaglia, N. Killeen, and M. Croft. 2001. OX40 promotes Bcl-x_L and Bcl-2 expression and is essential for long-term survival of CD4 T cells. *Immunity* 15: 445–455.
7. Lee, H.-W., S. J. Park, B. K. Choi, H. H. Kim, K. O. Nam, and B. S. Kwon. 2002. 4-1BB promotes the survival of $CD8^+$ T lymphocytes by increasing expression of Bcl-x_L and Bfl-1. *J. Immunol.* 169: 4882–4888.
8. Lens, S. M. A., K. Tesselaar, M. H. J. van Oers, and R. A. W. van Lier. 1998. Control of lymphocyte function through CD27-CD70 interactions. *Semin. Immunol.* 10: 491–499.
9. Gravestein, L. A., J. D. Nieland, A. M. Kruisbeek, and J. Borst. 1995. Novel mAbs reveal potent co-stimulatory activity of murine CD27. *Int. Immunol.* 7: 551–557.
10. Al-Shamkani, A., M. L. Birkeland, M. Puklavec, M. H. Brown, W. James, and A. N. Barclay. 1996. OX40 is differentially expressed on activated rat and mouse T cells and is the sole receptor for the OX40 ligand. *Eur. J. Immunol.* 151: 5261–5271.
11. Gramaglia, I., A. D. Weinberg, M. Lemon, and M. Croft. 1998. Ox-40 ligand: a potent costimulatory molecule for sustaining primary CD4 T cell responses. *J. Immunol.* 161: 6510–6517.
12. Pollok, K. E., Y.-J. Kim, Z. Zhou, J. Hurtado, K. K. Kim, R. T. Pickard, and B. S. Kwon. 1993. Inducible T cell antigen 4-1BB: analysis of expression and function. *J. Immunol.* 150: 771–781.
13. Cooper, D., P. Bansal-Pakala, and M. Croft. 2002. 4-1BB (CD137) controls the clonal expansion and survival of CD8 T cells in vivo but does not contribute to the development of cytotoxicity. *Eur. J. Immunol.* 32: 521–529.
14. Oshima, H., H. Nakano, C. Nohara, T. Kobata, A. Nakajima, N. A. Jenkins, D. J. Gilbert, N. G. Copeland, T. Muto, H. Yagita, and K. Okumura. 1998. Characterization of murine CD70 by molecular cloning and mAb. *Int. Immunol.* 10: 517–526.
15. Tesselaar, K., Y. Xiao, R. Arens, G. M. W. van Schijndel, D. H. Schuurhuis, R. Mebius, J. Borst, and R. A. W. van Lier. 2003. Expression of the murine CD27 ligand CD70 in vitro and in vivo. *J. Immunol.* 170: 33–40.
16. Stüber, E., M. Neurath, D. Calderhead, H. P. Fell, and W. Strober. 1995. Cross-linking of OX40 ligand, a member of the TNF/NGF cytokine family, induces proliferation and differentiation in murine splenic B cells. *Immunity* 2: 507–521.
17. Futagawa, T., H. Akiba, T. Kodama, K. Takeda, Y. Hosoda, H. Yagita, and K. Okumura. 2001. Expression and function of 4-1BB and 4-1BB ligand on murine dendritic cells. *Int. Immunol.* 14: 275–286.
18. Arens, R., K. Tesselaar, G. M. W. van Schijndel, P. A. Baars, S. T. Pals, P. Krimpenfort, J. Borst, M. H. J. van Oers, and R. A. W. van Lier. 2001. Constitutive CD27/CD70 interaction induces expansion of effector-type T cells and results in IFNγ-mediated B cell depletion. *Immunity* 15: 801–812.
19. Tesselaar, K., R. Arens, G. M. W. van Schijndel, P. A. Baars, M. A. van der Valk, J. Borst, M. H. J. van Oers, and R. A. W. van Lier. 2003. Lethal T cell immunodeficiency induced by chronic costimulation via CD27-CD70 interactions. *Nat. Immunol.* 4: 49–54.
20. Murata, K., M. Nose, L. C. Ndhlovu, T. Sato, K. Sugamura, and N. Ishii. 2002. Constitutive OX40/OX40 ligand interaction induces autoimmune-like diseases. *J. Immunol.* 169: 4628–4636.
21. Zhu, G., D. B. Flies, K. Tamada, Y. Sun, M. Rodriguez, Y.-X. Fu, and L. Chen. 2001. Progressive deletion of peripheral B lymphocytes in 4-1BB (CD137) ligand/I-Eα-transgenic mice. *J. Immunol.* 167: 2671–2676.
22. Maxwell, J. R., A. Weinberg, R. Prell, and A. T. Vella. 2000. Danger and OX40 receptor signaling synergize to enhance memory T cell survival by inhibiting peripheral deletion. *J. Immunol.* 164: 107–112.
23. Takahashi, C., R. S. Mittler, and A. T. Vella. 1999. 4-1BB is a bona fide CD8 T cell survival signal. *J. Immunol.* 162: 5037–5040.
24. Arens, R., K. Schepers, M. A. Nolte, M. F. van Oosterwijk, R. A. W. van Lier, T. N. M. Schumacher, and M. H. J. van Oers. 2004. Tumor rejection induced by CD70-mediated quantitative and qualitative effects on effector $CD8^+$ T cell formation. *J. Exp. Med.* 199: 1595–1605.
25. Hendriks, J., L. A. Gravestein, K. Tesselaar, R. A. W. van Lier, T. N. M. Schumacher, and J. Borst. 2000. CD27 is required for generation and long-term maintenance of T cell immunity. *Nat. Immunol.* 1: 433–440.
26. Tan, J. T., J. K. Whitmire, R. Ahmed, T. C. Pearson, and C. P. Larsen. 1999. 4-1BB ligand, a member of the TNF family, is important for the generation of antiviral CD8 T cell responses. *J. Immunol.* 163: 4859–4868.
27. DeBenedette, M., T. Wen, M. Bachmann, P. S. Ohashi, B. H. Barber, K. L. Stocking, J. J. Peschon, and T. Watts. 1999. Analysis of 4-1BB ligand (4-1BBL)-deficient mice and of mice lacking both 4-1BBL and CD28 reveals a role for 4-1BBL in skin allograft rejection and in the cytotoxic T cell response to influenza virus. *J. Immunol.* 163: 4833–4841.
28. Bertram, E. M., P. Lau, and T. Watts. 2002. Temporal segregation of 4-1BB versus CD28-mediated costimulation: 4-1BB ligand influences T cell numbers late in the primary response and regulates the size of the T cell memory response following influenza infection. *J. Immunol.* 168: 3777–3785.
29. Kopf, M., C. Ruedl, N. Schmitz, A. Gallimore, K. Lefrang, B. Ecabert, B. Odermatt, and M. F. Bachmann. 1999. OX40-deficient mice are defective in Th cell proliferation but are competent in generating B cell and CTL responses after virus infection. *Immunity* 11: 699–708.
30. Chen, A. I., A. J. McAdam, J. E. Buhlmann, S. Scott, M. L. Lupher, E. A. Greenfield, P. R. Baum, W. C. Fanslow, D. M. Calderhead, G. J. Freeman, and A. H. Sharpe. 1999. Ox40-ligand has a critical costimulatory role in dendritic cell:T cell interactions. *Immunity* 11: 689–698.
31. Murata, K., N. Ishii, H. Takano, S. Miura, L. C. Ndhlovu, M. Nose, T. Noda, and K. Sugamura. 2000. Impairment of antigen-presenting cell function in mice lacking expression of OX40 ligand. *J. Exp. Med.* 191: 365–374.
32. Gramaglia, I., A. Jember, S. D. Pippig, A. D. Weinberg, N. Killeen, and M. Croft. 2000. The OX40 costimulatory receptor determines the development of CD4 memory by regulating primary clonal expansion. *J. Immunol.* 165: 3043–3050.
33. Humphreys, I. R., G. Walzl, L. Edwards, A. Rae, S. Hill, and T. Hussell. 2003. A critical role for OX40 in T cell-mediated immunopathology during lung infection. *J. Exp. Med.* 8: 1237–1242.
34. Bansal-Pakala, P., B. S. Halteman, M. H.-Y. Cheng, and M. Croft. 2004. Costimulation of CD8 T-cell responses by OX40. *J. Immunol.* 172: 4821–4825.
35. Dawicki, W., E. M. Bertram, A. H. Sharpe, and T. H. Watts. 2004. 4-1BB and OX40 act independently to facilitate robust CD8 and CD4 recall responses. *J. Immunol.* 173: 5944–5951.
36. Salek-Ardakani, S., J. Song, B. S. Halteman, A. G. Jember, H. Akiba, H. Yagita, and M. Croft. 2003. OX40 (CD134) controls memory T helper 2 cells that drive lung inflammation. *J. Exp. Med.* 198: 315–324.

37. Haanen, J. B. A., M. Wolkers, A. M. Kruisbeek, and T. N. M. Schumacher. 1999. Selective expansion of cross-reactive CD8$^+$ memory T cells by viral variants. *J. Exp. Med.* 190: 1319–1328.
38. Xiao, Y., J. Hendriks, P. Langerak, H. Jacobs, and J. Borst. 2004. CD27 is acquired by primed B cells at the centroblast stage and promotes germinal center formation. *J. Immunol.* 172: 7432–7441.
39. Ward, C. L., M. H. Dempsey, C. J. A. Ring, R. E. Kempson, L. Zhang, D. Gor, B. W. Snowden, and M. Tisdale. 2004. Design and performance testing of quantitative real time PCR assays for influenza A and B viral load measurement. *J. Clin. Virol.* 29: 179–188.
40. Belz, G. T., W. Xie, and P. C. Doherty. 2001. Diversity of epitope and cytokine profiles for primary and secondary influenza A virus-specific CD8$^+$ T cell responses. *J. Immunol.* 166: 4627–4633.
41. Bertram, E. M., W. Dawicki, B. Sedgmen, J. L. Bramson, D. H. Lynch, and T. H. Watts. 2004. A switch in costimulation from CD28 to 4-1BB during primary versus secondary CD8 T cell response to influenza in vivo. *J. Immunol.* 172: 981–988.
42. Rowley, T. F., and A. Al-Shamkhani. 2004. Stimulation by soluble CD70 promotes strong primary and secondary CD8$^+$ cytotoxic T cell responses in vivo. *J. Immunol.* 172: 6039–6046.
43. Van Stipdonk, M. J. B., E. E. Lemmens, and S. P. Schoenberger. 2001. Naive CTLs require a single brief period of antigen stimulation for clonal expansion and differentiation. *Nat. Immunol.* 4: 361–365.
44. Kaech, S. M., and R. Ahmed. 2001. Memory CD8$^+$ T cell differentiation: initial antigen encounter triggers a developmental program in naive cells. *Nat. Immunol.* 2: 415–422.
45. Schluns, K. S., and L. Lefrancois. 2003. Cytokine control of memory T-cell development and survival. *Nat. Rev. Immunol.* 3: 269–279.
46. Janssen, E. M., E. E. Lemmens, T. Wolfe, U. Christen, M. G. von Herrath, and S. Schoenberger. 2003. CD4$^+$ T cells are required for secondary expansion and memory in CD8$^+$ T lymphocytes. *Nature* 421: 852–856.
47. Shedlock, D. J., and H. Shen. 2003. Requirement for CD4 T cell help in generating functional CD8 T cell memory. *Science* 300: 337–339.
48. Sun, J. C., and M. J. Bevan. 2003. Defective CD8 T cell memory following acute infection without CD4 T cell help. *Science* 300: 339–342.

nature genetics

Positional identification of *TNFSF4*, encoding OX40 ligand, as a gene that influences atherosclerosis susceptibility

Xiaosong Wang[1,8], Massimiliano Ria[2,8], Peter M Kelmenson[1], Per Eriksson[2], David C Higgins[1], Ann Samnegård[2], Christina Petros[1], Jarod Rollins[1], Anna M Bennet[3], Björn Wiman[4], Ulf de Faire[3,5], Charlotte Wennberg[6], Per G Olsson[6], Naoto Ishii[7], Kazuo Sugamura[7], Anders Hamsten[2], Kristina Forsman-Semb[6], Jacob Lagercrantz[2] & Beverly Paigen[1]

***Ath1* is a quantitative trait locus on mouse chromosome 1 that renders C57BL/6 mice susceptible and C3H/He mice resistant to diet-induced atherosclerosis. The quantitative trait locus region encompasses 11 known genes, including *Tnfsf4* (also called *Ox40l* or *Cd134l*), which encodes OX40 ligand. Here we report that mice with targeted mutations of *Tnfsf4* had significantly ($P \leq 0.05$) smaller atherosclerotic lesions than did control mice. In addition, mice overexpressing *Tnfsf4* had significantly ($P \leq 0.05$) larger atherosclerotic lesions than did control mice. In two independent human populations, the less common allele of SNP rs3850641 in *TNFSF4* was significantly more frequent ($P \leq 0.05$) in individuals with myocardial infarction than in controls. We therefore conclude that *Tnfsf4* underlies *Ath1* in mice and that polymorphisms in its human homolog *TNFSF4* increase the risk of myocardial infarction in humans.**

Atherosclerosis is the pathological basis for coronary artery disease, the leading cause of death in the developed world. It is a complex trait regulated by many genes, environmental factors and interactions among them. Genes controlling atherogenesis can be identified either through clinical and biochemical studies of occasional natural mutations in humans and other animals or by genetic mapping. Nearly two decades ago, we surveyed the susceptibility of ten inbred mouse strains to diet-induced atherosclerosis[1] and found that C57BL/6 (B6) mice are susceptible whereas C3H/He (C3H) and BALB/c mice are resistant. By comparing the atherosclerotic lesions of BXH and BXC recombinant inbred lines, we identified the first atherosclerosis susceptibility locus, *Ath1* (atherosclerosis susceptibility 1), which we mapped to chromosome (Chr) 1 (refs. 2,3). Later, using congenic strains, we narrowed *Ath1* to a 0.66-cM region on Chr 1 (ref. 4) containing 11 known genes. Three of them (peroxiredoxin 6, *Prdx6*; Fas ligand, *Tnfsf6*, also called *Fasl*; and OX40 ligand, *Tnfsf4*) have known

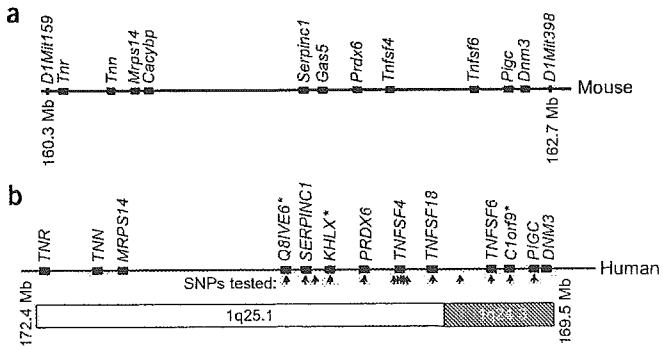

Figure 1 Genes in the *Ath1* region. Genes in (**a**) the mouse *Ath1* region and (**b**) the human homologous chromosome segment between 1q24.3 to 1q25.1 were retrieved from the Ensembl database and Celera Discovery System. Arrows indicate established and putative (*) genes tested in human SNP association studies; each arrow represents one tested SNP. *Tnr* and *TNR*, tenascin R; *Tnn* and *TNN*, tenascin N; *Mrps14* and *MRPS14*, mitochondrial ribosomal protein S14; *Cacybp*, calcyclin binding protein; *Serpinc1* and *SERPINC1*, serine (or cysteine) proteinase inhibitor, clade C, member 1; *Gas5*, growth arrest specific 5; *KHLX*, Kelch-like protein X; *Prdx6* and *PRDX6*, peroxiredoxin 6; *Tnfsf6* and *TNFSF6*, tumor necrosis factor ligand superfamily member 6 (Fas ligand); *C1orf9*, chromosome 1 open reading frame 9; *Pigc* and *PIGC*, phosphatidylinositol glycan, class C; *Dnm3* and *DMN3*, dynamin 3.

[1]The Jackson Laboratory, 600 Main Street, Bar Harbor, Maine 04609, USA. [2]Atherosclerosis Research Unit, King Gustaf V Research Institute, Department of Medicine; [3]Division of Cardiovascular Epidemiology, Institute for Environmental Medicine; [4]Division of Clinical Chemistry and Blood Coagulation, Department of Surgical Sciences; and [5]Department of Cardiology; Karolinska Institute, Karolinska Hospital, Stockholm, Sweden. [6]Department of Molecular Biology, AstraZeneca R&D, Mölndal, Sweden. [7]Department of Microbiology and Immunology, Tohoku University Graduate School of Medicine, Sendai, Japan. [8]These authors contributed equally to this work. Correspondence should be addressed to X.W. (xw@jax.org).

Published online 6 March 2005; doi:10.1038/ng1524

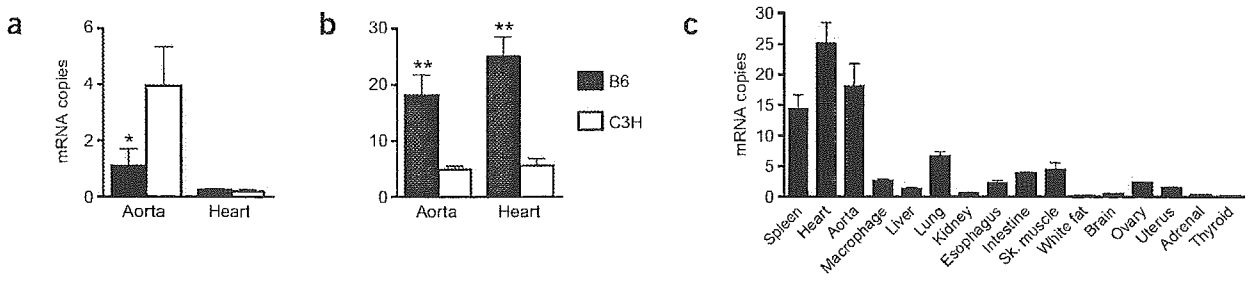

Figure 2 mRNA expression of *Tnfsf6* and *Tnfsf4*. Comparison of mRNA expression of *Tnfsf6* (**a**) and *Tnfsf4* (**b**) in aorta and heart from 10-week-old female B6 and C3H mice fed chow. (**c**) mRNA expression of *Tnfsf4* in tissues from 10-week-old female B6 mice. The number of copies of each mRNA relative to 1,000 copies of β-actin mRNA is shown on the *y* axis. Each bar represents mean ± s.e.m. of three mice. $^*P < 0.05$, $^{**}P < 0.01$ compared with the expression in the same tissue from C3H mice.

functions that may affect atherogenesis. Because many lines of evidence suggest that oxidative stress and oxidative modification of low-density lipoprotein (LDL) participate in atherogenesis, PRDX6 (also called antioxidant protein 2), an antioxidant enzyme that protects mice against oxidative stress[5], may protect against atherosclerosis. We previously tested *Prdx6* but found that mice overexpressing PRDX6 (ref. 6) and mice deficient in PRDX6 (ref. 7) are as susceptible to diet-induced atherosclerosis as are their respective controls. Therefore, we excluded *Prdx6* as a candidate for underlying *Ath1*.

Here we test *Tnfsf6* and *Tnfsf4* as candidates for underlying *Ath1*. The Fas–Fas ligand–caspase death-signaling pathway is activated in atherosclerotic lesions and mediates vascular apoptosis during the development of atherosclerosis[8]. OX40 ligand (OX40L) is expressed on activated B cells, endothelial cells, macrophages, dendritic cells and some activated T cells. It generates costimulatory signals by interacting with OX40 on T lymphocytes, and it enhances the proliferation and differentiation of T lymphocytes and the development and survival of memory $CD4^+$ T cells[9]. Because many *in vivo* studies suggest that T lymphocytes promote atherosclerosis[10], OX40L, by enhancing T cell functions, might be proatherogenic. Therefore, we compared diet-induced atherosclerosis in mice deficient in either *Tnfsf6* or *Tnfsf4* and in their respective controls. We obtained evidence that *Tnfsf4* affected atherosclerosis in mice and then tested *TNFSF4* in a hypothesis-driven association study in humans. We found that polymorphisms in human *TNFSF4* were associated with risk of myocardial infarction and severity of coronary artery stenosis.

RESULTS

Genes in mouse *Ath1* and its human homologous regions

The Ensembl and Celera Discovery System databases indicated that the 2.4-Mb (0.66-cM) mouse *Ath1* region (between *D1Mit159* and *D1Mit398*) contains 11 known genes (**Fig. 1a**). The homologous region in humans, between 1q24.3 and 1q25.1, contains ten known genes and three putative genes (*Q8IVE6*, *KHLX* and *C1orf9*; **Fig. 1b**). Two of the known mouse genes (*Cacybp* and *Gas5*) do not have known human gene counterparts, and one of the known human genes (*TNFSF18*) does not have a known mouse gene counterpart.

Sequence and expression analysis of *Tnfsf6* and *Tnfsf4*

The gene underlying a quantitative trait locus (QTL) should have either a coding-sequence difference that changes the function of the protein it encodes or a regulatory-sequence difference that causes a difference in gene expression between the two parental strains. The coding sequences of *Tnfsf6* and *Tnfsf4* were identical in B6 and C3H mice. We compared *Tnfsf4* and *Tnfsf6* mRNA expression in aortas and hearts of B6 and C3H mice. Aortic expression of *Tnfsf6* mRNA was significantly higher ($P < 0.05$) in C3H than in B6 mice (**Fig. 2a**).

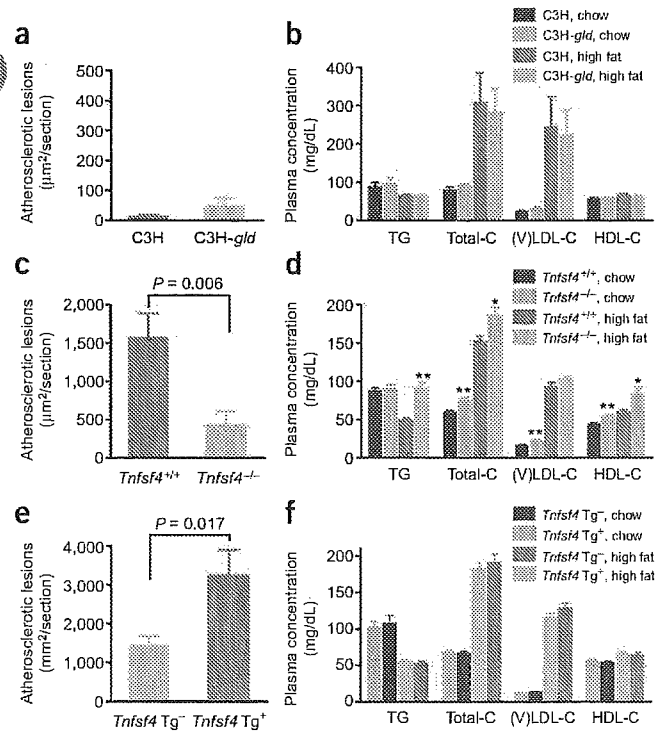

Figure 3 Diet-induced atherosclerosis and plasma lipid levels in *Tnfsf6* or *Tnfsf4* mutant mice, in transgenic mice overexpressing *Tnfsf4* and in their respective controls. Ten-week-old females were fed a high-fat diet for either 13 weeks (mutant mice and their controls) or 16 weeks (transgenic mice and their controls), after which their hearts and aortas were collected and atherosclerosis lesions in aortic roots were measured. Plasma lipid levels were measured before (chow) and after mice had fed on high-fat diet. (**a**,**c**,**e**) Diet-induced atherosclerosis in C3H *Tnfsf6*^{gld} (CH3-*gld*; $n = 12$), *Tnfsf4*$^{-/-}$ ($n = 12$) and *Tnfsf4* transgenic (Tg^+; $n = 14$) mice, respectively, and their controls (C3H ($n = 12$), *Tnfsf4*$^{+/+}$ ($n = 12$) and *Tnfsf4* nontransgenic (Tg^-; $n = 14$), respectively). (**b**,**d**,**f**) Plasma lipid levels in C3H *Tnfsf6*^{gld}, *Tnfsf4*$^{-/-}$ and *Tnfsf4* transgenic mice, respectively, and their controls. TG, triglycerides; Total-C, total cholesterol; (V)LDL-C, very-low-density lipoprotein and LDL cholesterol combined; HDL-C, HDL cholesterol. *P* values were calculated with Student's *t*-test. $^*P < 0.05$, $^{**}P < 0.01$ compared with wild-type mice on the same diet.

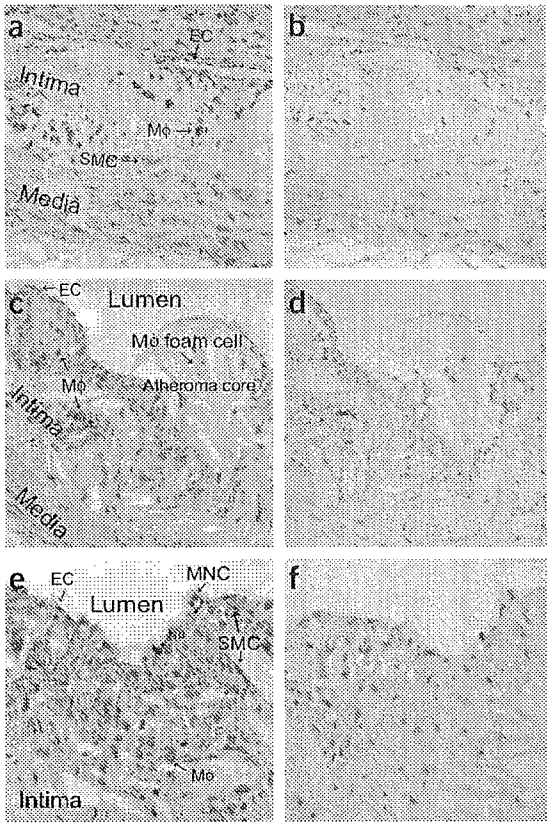

Figure 4 Immunohistochemical localization of OX40L protein in mouse atherosclerotic lesions. Segments of aortic arches from 6-month-old female *Apoe*-deficient mice were fixed in Bouin's solution, and OX40L was detected with antibody to OX40L by using the avidin–biotin–horseradish peroxidase complex method. Staining of OX40L (**a**,**c**,**e**; each from a separate mouse) was compared with corresponding serial slides stained with nonimmune IgG instead of IgG antibody to mouse OX40L (**b**,**d**,**f**). EC, endothelial cell; Mφ, macrophage; MNC, mononuclear cell; SMC, smooth muscle cell.

Aortic and heart expression of *Tnfsf4* mRNA was 3.7 and 4.5 times higher, respectively, in B6 than in C3H mice (**Fig. 2b**). Because many lines of evidence suggest that *Tnfsf4* underlies *Ath1*, we sequenced 5 kb upstream of exon 1 of *Tnfsf4* in B6 and C3H mice. We found single-nucleotide differences at two positions and single-nucleotide deletions at six locations in one of the two strains (**Supplementary Table 1** online), differences that could change promoter activities and *Tnfsf4* mRNA expression levels. To explore further the possibility that *Tnfsf4* underlies *Ath1*, we measured its mRNA expression in 16 tissues from female B6 mice. Expression was relatively high in spleen, aorta and heart; intermediate in lung, intestine and skeletal muscles; and relatively low in other tissues (**Fig. 2c**).

In vivo evidence that *Tnfsf4* underlies *Ath1*

When fed either chow or a high-fat diet, female C3H mice with an inactivating mutation in *Tnfsf6* (C3H *Tnfsf6*^{gld}) and control mice were both very resistant to diet-induced atherosclerosis (**Fig. 3a**), and they had comparable ($P > 0.05$) plasma lipid levels (**Fig. 3b**). In contrast, female *Tnfsf4* knockout mice (*Tnfsf4*$^{-/-}$) fed a high-fat diet for 13 weeks had significantly smaller (3.7 times, $P = 0.006$) atherosclerotic lesions than did controls (*Tnfsf4*$^{+/+}$; **Fig. 3c**). Like *Prdx6*$^{-/-}$ mice[7], *Tnfsf4*$^{-/-}$ mice fed either chow or a high-fat diet had higher levels of plasma total cholesterol and high-density lipoprotein (HDL) cholesterol than did controls (**Fig. 3d**). On the other hand, female transgenic mice overexpressing *Tnfsf4* had significantly larger (2.3 times, $P = 0.017$) atherosclerotic lesions than did controls (**Fig. 3e**). Transgenic and nontransgenic mice had similar plasma lipid levels (**Fig. 3f**).

Table 1 Characteristics of the study groups

	SCARF		SHEEP	
	Affected	Control	Affected	Control
n	401	392	1,213	1,561
Gender (female/male)	71/330	69/323	361/852	507/1,054
Age (y)	52 ± 6	53 ± 5	59 ± 2	60 ± 2
Smokers, % (current/previous)	18/57	23/37	49/26	29/30
Type 2 diabetes (%)	10.7	0*	12.1	4.6*
BMI (kg m^{-2})	27.4 ± 0.2	26.5 ± 0.2*	26.6 ± 0.1	25.5 ± 0.1*
LDL cholesterol (mmol l^{-1})	3.23 ± 0.05	3.52 ± 0.05*	4.22 ± 0.02	3.96 ± 0.02*
HDL cholesterol (mmol l^{-1})	1.10 ± 0.02	1.41 ± 0.02*	1.08 ± 0.01	1.29 ± 0.01*
Plasma triglycerides (mmol l^{-1})	1.66 ± 0.03	1.21 ± 0.02*	1.76 ± 0.01	1.32 ± 0.01*

Values are mean ± s.e.m.
*$P < 10^{-4}$ compared with the affected individuals in the same study group.

OX40L protein is expressed in mouse atherosclerotic lesions

We detected OX40L protein in aortas from *Apoe*-deficient mice by immunohistochemistry. We used *Apoe*-deficient mice for several reasons. First, *Ath1* may also be responsible for the difference in atherosclerosis susceptibility between *Apoe*-deficient B6 mice and *Apoe*-deficient C3H mice[11]. Second, *Tnfsf4* knockout mice with *Apoe* deficiency had smaller atherosclerotic lesion than did control *Apoe*-deficient mice (X.W. and B.P., unpublished data), suggesting that *Ath1* regulates atherogenesis in the *Apoe*-deficient mouse model. Third, cells from these mice are abundant and easy to identify. Immunohistochemical analysis of atherosclerotic lesions from B6 *Apoe*-deficient mice showed OX40L-specific staining in endothelial cells of both relatively normal (**Fig. 4a**) and plaque-ridden (**Fig. 4c**,**e**) aortas and in medial smooth muscle cells (**Fig. 4a**). Inside the lesions, considerable OX40L staining was detected in macrophages, smooth muscles and small mononuclear cells (lymphocytes). OX40L was expressed on cell membranes. In contrast, little OX40L staining was detected in the extracellular areas, including the necrotic atheromatous core (**Fig. 4c**). Serial slides stained with nonimmune serum yielded no specific staining (**Fig. 4b**,**d**,**f**). Little OX40L was expressed in normal aorta (data not shown).

A *TNFSF4* SNP associated with risk of myocardial infarction

Because our results in mice indicated that *Tnfsf4* affected atherosclerosis, we examined polymorphisms in *TNFSF4* in humans in a hypothesis-driven association study. The characteristics of the study groups are shown in **Table 1**. In the first population, the Stockholm Coronary Atherosclerosis Risk Factor (SCARF) study, we tested *TNFSF4* in 401 individuals with myocardial infarction and 392 controls, obtaining complete data from 359 affected individuals and 382 controls (individuals treated with statins were excluded). As a group, the affected individuals included significantly ($P < 0.0001$) more previous smokers and individuals with type 2 diabetes, had higher body mass index (BMI) and plasma triglyceride concentrations